



STANFORD GEOTHERMAL PROGRAM
STANFORD UNIVERSITY

STANFORD, CALIFORNIA 94305

Stanford Geothermal Program
Interdisciplinary Research in
Engineering and Earth Sciences
STANFORD UNIVERSITY
Stanford, California

SGP-TR-72

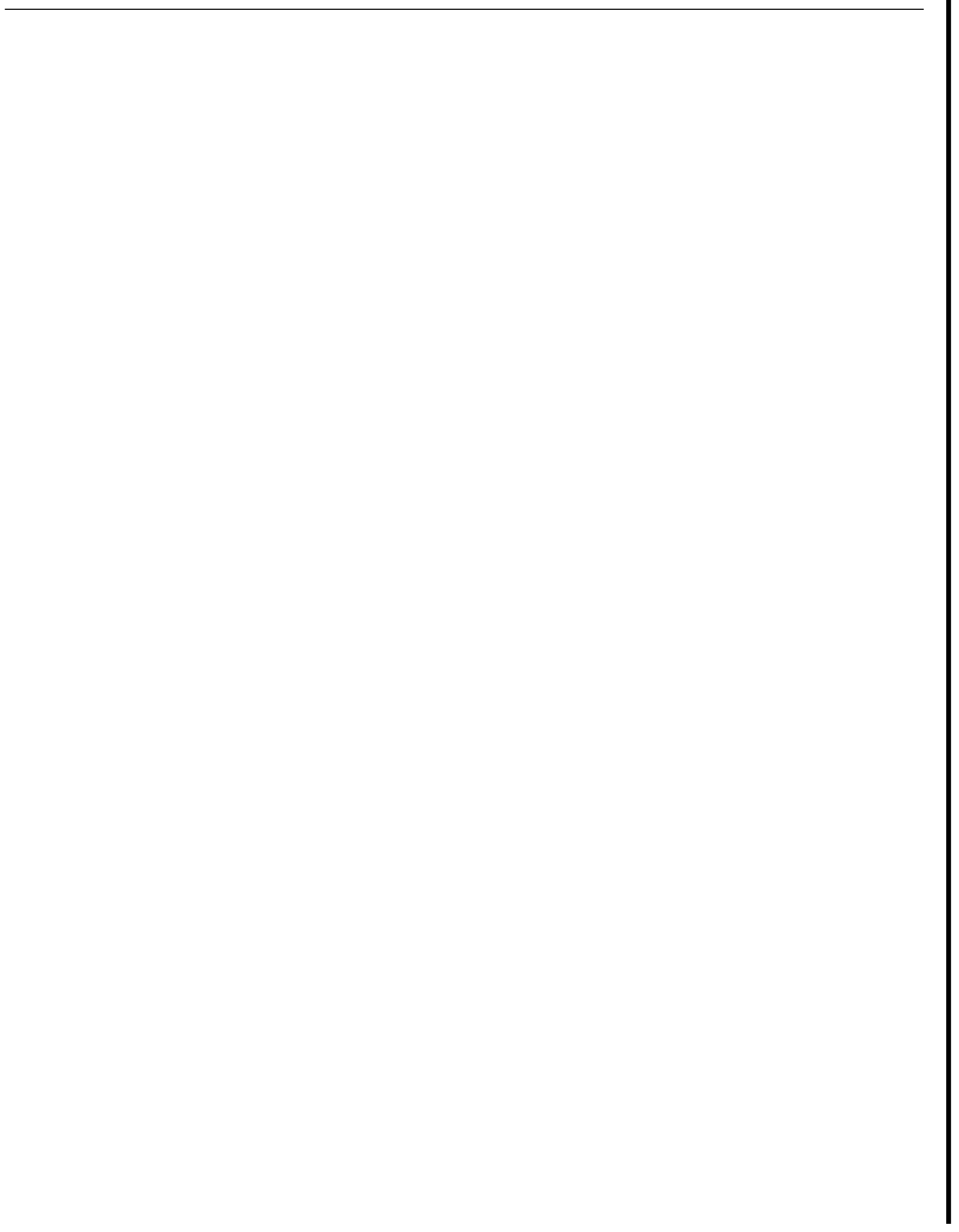
A RESERVOIR ENGINEERING
ANALYSIS OF A VAPOR-DOMINATED
GEOTHERMAL FIELD

By

John Forrest Dee

June 1983

Financial support was provided through the Stanford Geothermal Program under Department of Energy Contract No. DE-AT03-80SF11459 and by the Department of Civil Engineering, Stanford University.



ABSTRACT

A model has been developed to predict both reserves and deliverability in a "vapor-dominated" geothermal field. The data used are fictitious, although, their general character is similar to that seen in real fields.

This study, initiated in June 1982 and completed in May 1983, is a continuation of a previous one by William E. Brigham. The purpose of this report is to show that the empirical lumped parameter model is effective in describing pressure drawdown behavior in a vapor dominated geothermal reservoir, and to demonstrate how addition of deliverability information can be incorporated in the Brigham model.

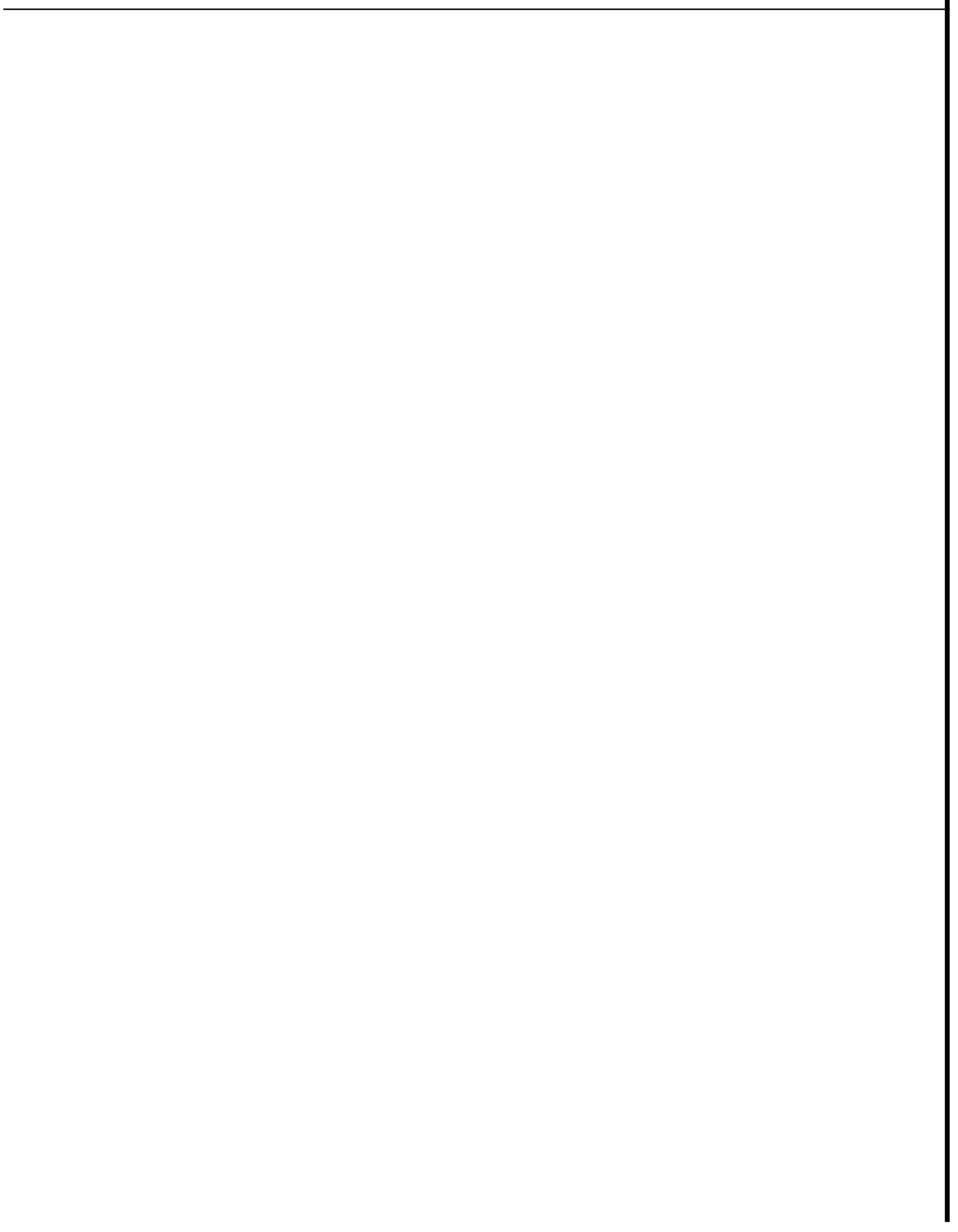
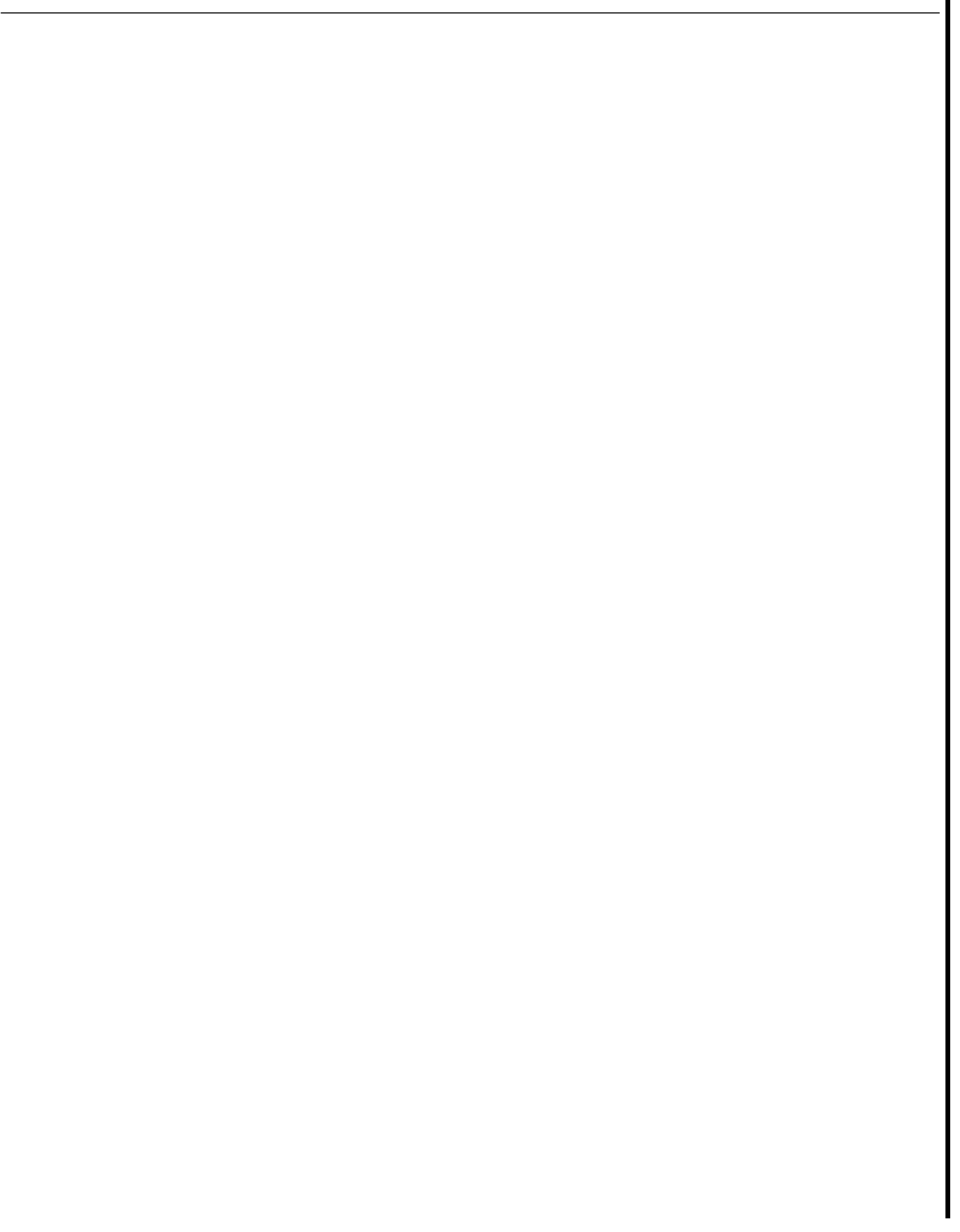


TABLE OF CONTENTS

	<u>Page</u>
ACKNOWLEDGEMENTS	is
ABSTRACT	iif
TABLE OF CONTENTS	iv
LIST OF TABLES	v
LIST OF FIGURES	vi
1. INTRODUCTION	1
2. DESCRIPTION OF THE RESERVOIR	1
3. PRESSURE AND PRODUCTION DATA	e
4. PREVIOUS HISTORY MATCHING EFFORTS	7
5. RELATING $w(p/z)$ TO FLOW RATE	14
6. CURRENT RESERVOIR HISTORY MATCHING EFFORTS	18
7. ANALYSIS OF FRICTIONAL FLOW CONSTANTS	21
8. ANALYSIS OF UNIT F BEHAVIOR	22
9. RESERVOIR PRESSURE MATCH AND EXTRAPOLATION	23
10. DELIVERABILITY AND FUTURE PRODUCING RATES	26
11. CONCLUSIONS	42
NOMENCLATURE	45
REFERENCES	47
APPENDIX: COMPUTER PROGRAM	48



LIST OF TABLES

<u>Table</u>		<u>Page</u>
1	Cumulative Production and Average p/Z	2
2	Real Gas Compressibility Factors	3
3	Gross Equivalent Flow Rates (i)	12
4	Gross Equivalent Flow Rates (ii)	13
5	Sensitivity of Frictional Flow Constant. C	21
6	Summary of Projected New Unit Behavior	25
7	Future Production and Equivalent Flow Rates	27
8	Deliverability Data	31
9	Deliverability Data (All Units Combined)	32
10	Projections of Flow Rate and Pressure	40

LIST OF FIGURES

<u>Figure</u>		<u>Page</u>
1	Compressibility Factor Extrapolation	4
2	Gas Depletion Integral	5
3	Dimensionless Pressure Change. Linear Aquifers ...	7
4	Pressure Production History Match (i)	19
5	Pressure Production History Match (ii)	24
6	Deliverability Analysis (Unit A)	33
7	Deliverability Analysis (Unit B)	34
8	Deliverability Analysis (Unit C)	35
9	Deliverability Analysis (Unit D)	36
10	Deliverability Analysis (All Units Combined)	37
11	Projected Flow Rates	41
12	Projected p/z Decline	44

1. INTRODUCTION

This report is an extension of the Brigham model to fictitious data for a vapor-dominated geothermal field. The purpose of the study is to develop a simplified model to match past performance of the reservoir and to predict future production rates and ultimate reserves. A lumped parameter model was developed for the reservoir that is similar to the model developed by Brigham and Neri (1979) for the Gabbro zone, and a deliverability model was developed to predict the life and future producing rate declines of the reservoir. This report presents the development and results of this geothermal reservoir analysis.

2. DESCRIPTION OF THE RESERVOIR

During the course of production from the reservoir, flow rates and pressures have declined during several periods during which the number of wells has remained approximately constant. This suggests that the reservoir is undergoing depletion. It is reasonable to assume that there exists a boiling water zone deep in the reservoir. The rock matrix between this deep zone and the producing zone consists of relatively tight vertical fractures. The model presented in this report is based on this concept of a deep boiling water zone which supplies steam to a shallower producing horizon. The pressure drawdown measured in the producing zone is a combination of a pressure drop due to depletion of the boiling water and a pressure drop due to frictional

flow of the steam as it rises through these vertical fractures. Using analytical linear flow equations to match the vertical frictional pressure drop, the pressures measured in the producing zone have been closely matched. The development of the history match will be presented in the following sections.

3. PRESSURE AND PRODUCTION DATA

The hypothetical pressure and production data used for this study are presented in Table 1 on the following page. The value zero for the number of months corresponds to the beginning of production.

Table 1

CUMULATIVE PRODUCTION & AVERAGE p/Z
Units A-C, D, E, and F

<u>Months</u>	<u>Cumulative Production</u> (10 ⁹ lbs.)		<u>p/Z</u>
	<u>Gross</u>	<u>Net</u>	
0	0.0	0.0	707
71	31.0	31.0	706
77	33.8	33.8	705
93	44.4	44.4	704
107	57.0	57.0	698
117	66.8	66.8	696
132	84.3	80.1	695
144	105.3	98.3	686
154	131.9	120.0	672
167	166.3	148.8	660
175	189.4	167.0	643
182	211.1	184.5	626
192	244.7	209.7	598
200	272.0	231.4	585
206	291.7	248.3	579
212	311.9	262.9	574
220	336.4	281.8	568
226	356.7	297.2	561
235	389.6	321.7	546
249	441.4	360.2	533

The p/Z data listed in Table 1 are average p/Z values for the entire reservoir. The Z -factor data were calculated assuming isothermal conditions ($480^\circ F$) exist in the reservoir. The PVT data for steam were taken from Keenan and Keyes (1969), and the resulting Z -factors are listed in Table 2. Note that for pressures above 570 psia, the steam condenses at $480^\circ F$. The Z -factors at pressures above this value were calculated by extrapolating the values at the lower pressures. This extrapolation is shown in Fig. 1. Of course, these Z -factors are not real. They merely result from the fact that the data have been altered. These synthetic values of Z do not affect the validity of the concepts used.

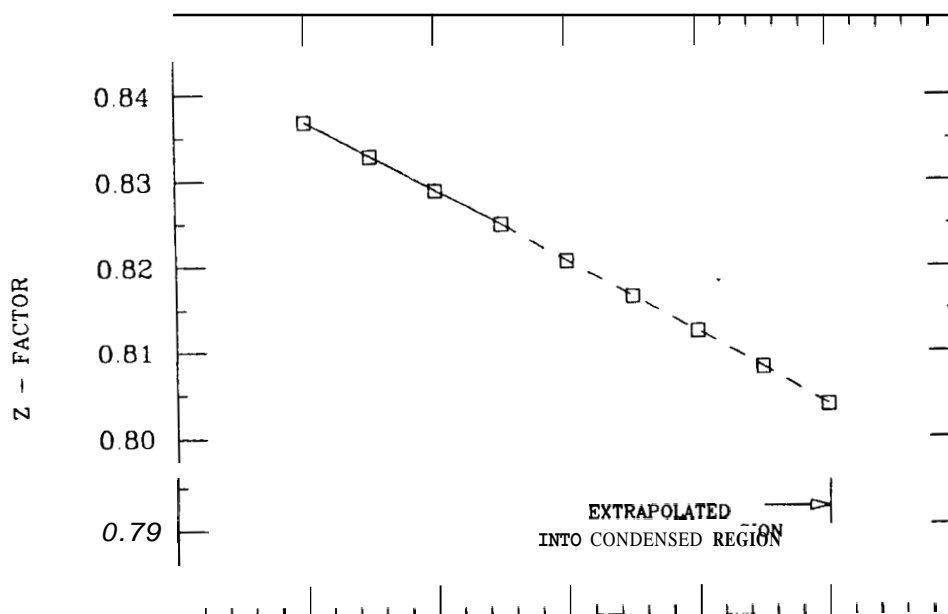
Table 2

REAL GAS COMPRESSIBILITY FACTORS FOR STEAM AT $480^\circ F$

<u>Pressure</u> <u>(psia)</u>	<u>Z</u>	<u>Pressure</u> <u>(psia)</u>	<u>Z</u>
620	0.8038	460	0.8666
600	0.8124	440	0.8736
580	0.8207	420	0.8805
560	0.8289	400	0.8872
540	0.8368	380	0.8938
520	0.8446	360	0.9003
500	0.8521	340	0.9067
480	0.8594		

In Fig. 2, $\Delta(p/Z)$ has been graphed against area to determine average p/Z values. The $\Delta(p/Z)$ data were obtained from pressure contour maps. By graphically integrating the resulting curves and dividing the

result by the total area of the reservoir, average values of $\Delta(p/Z)$ were calculated. The first curve near the origin represents the 71 month data in Table 1, while the last curve represents the 249 month data of Table 1. Notice there are 19 data points of reduced p/Z in Table 1, while there are only 18 curves in Fig. 2. This is because the data at 117 months and 132 months were nearly identical. The values from these integrated curves were then subtracted from 707.0, the initial p/Z value, to determine the average values at the various dates. As a note, we have used a figure of 2900 acres for the total drainage area of the field. The method of determination of average p/Z outlined above is the easiest and most accurate method of determining average values.



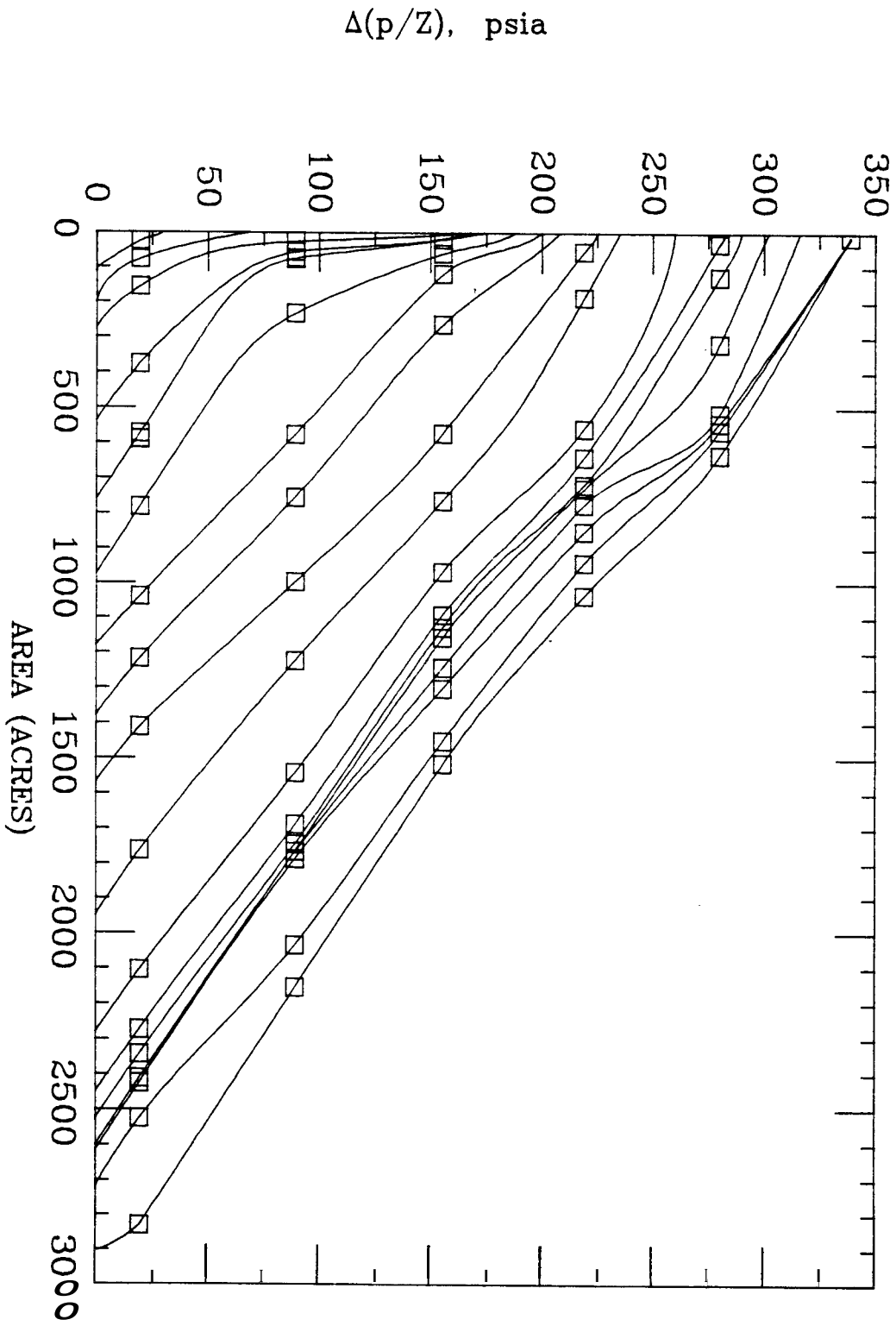


FIGURE 2
 GAS DEPLETION INTEGRAL
 $\Delta(p/Z)$ VS AREA FOR PRESSURE CELL

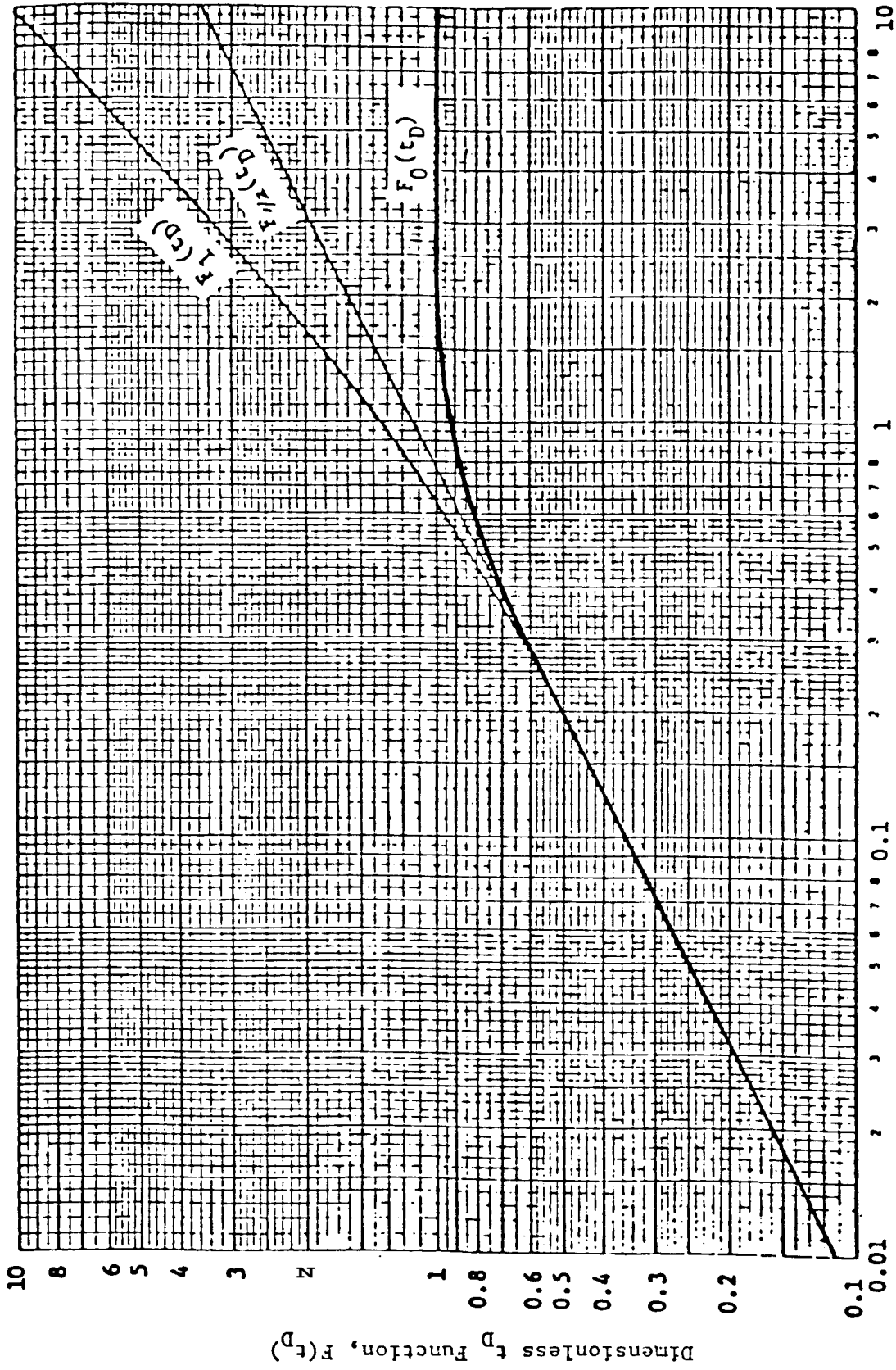
4. PREVIOUS HISTORY MATCHING EFFORTS

In their study of the Gabbro Zone, Brigham and Neri(1979) combined the standard gas material balance with an empirical power law equation to describe pressure drawdown in the producing zone. The empirical power law equation was derived to model the transient pressure behavior that existed between the top of the reservoir, where the wells are completed, and the constant pressure boiling water interface deep in the reservoir. We would like to review the development of this empirical equation because of its importance to the model.

To derive an equation for the pressure drop from the deep boiling zone through the fractured zone to the producing horizon, we can envision that the flow geometry is approximately linear. This is transient flow, and therefore the magnitude of the pressure drop will depend on the terms in the p_D function for linear flow, and the timing of the pressure transient will depend on the terms in the t_D function. Analytical solutions for such problems have been published by Millet (1962) and by Nabor and Barham (1964). Nabor and Barham's solutions are summarized in Fig. 3, where their term $F(t_D)$ is the p_D function for linear flow at a constant rate inner boundary condition.

The three curves shown in Fig. 3 represent three different outer boundary conditions; that is, the boundary condition at the boiling water interface. The system that most closely approximates a boiling water interface is the constant pressure boundary, represented by the $F_0(t_D)$ curve. This is marked more heavily in Fig. 3. This curve also presumes an inner boundary condition of constant flow rate. For the

FIGURE 3



Dimensionless Time, t_D

DIMENSIONLESS PRESSURE CHANGE AND EFFLUX FUNCTIONS, LINEAR AQUIFERS
 (After Nabor and Barham, Trans., AIME (1964), 231, 561)

actual variable flow rate, it is necessary to use superposition to calculate the transient pressure drop. The appropriate superposition equation is the following:

$$\frac{kA \Delta p}{\mu L} = q_1 p_D(t_D) + (q_2 - q_1) p_D(t_D - \Delta t_{D1}) + (q_3 - q_2) p_D(t_D - \Delta t_{D1} - \Delta t_{D2}) + (q_4 - q_3) p_D(t_D - \Delta t_{D1} - \Delta t_{D2} - \Delta t_{D3}) + \dots + \quad (1)$$

where :

$p_D(t_D)$ = the value of $F_o(t_D)$ from Fig. 3 at a time equal to t_D .

q_n = the flow rate during the nth time period.

Let us study the $F_o(t_D)$ curve in Fig. 3 in detail. A good approximation to this curve is to assume that p_D is proportional to the square root of time until $t_D = 0.785$ and to assume it is a constant equal to 1.00 after $t_D = 0.785$. The maximum error using the approximation is only about 10%. This can also be seen from the analytical solution to the linear flow equation for an infinite system:

$$\Delta p = \frac{q \mu}{k b h} \sqrt{\frac{kt}{\pi \phi \mu c_t}} \quad (2)$$

In Eq. 2, Δp is proportional to the square root of time. Once the outer boundary is felt by the pressure transient, Eq. 2 no longer applies, and at long times Δp will remain constant for a constant pressure outer boundary.

In most real systems, we do not know the parameters in t_D well enough to be able to relate the real time to t_D ; however, we can assume a value for the real time that is equivalent to $t_D = 0.785$ and observe how this affects Eq. 1. In this report, we will refer to this time as the "lag time." This phrase was chosen for it is meant to imply the time required to reach effective steady-state flow. Therefore, if we assume a lag time of 30 months, then the relationship between t_D and t can be expressed as follows:

$$\frac{t_D}{0.785} = \frac{t}{30} \quad (3)$$

To determine the effect of the lag time and the above approximations on the superposition equation, let us for illustration assume six time periods of varying lengths as follows: 15 mo., 10 mo., 10 mo., 10 mo., 5 mo., and 10 mo., for a total of 60 months. From Eq. 1, we see that the pressure drawdown due to the first rate is felt for the entire 60 months, the drawdown due to the second rate is felt for 45 months, and so on. The result is Eq. 4 :

$$\begin{aligned} \frac{k A \Delta p}{\mu L} = & q_1 p_D(60) + (q_2 - q_1) p_D(45) + (q_3 - q_2) p_D(35) \\ & + (q_4 - q_3) p_D(25) + (q_5 - q_4) p_D(15) + (q_6 - q_5) p_D(10) \end{aligned} \quad (4)$$

where :

$p_D(25)$ = the value of $F_o(t_D)$ from Fig. 3 at a time equal to 25 months. Other $p_D(t)$ values are defined similarly.

Because our assumed lag time is 30 months, the values for $p_D(t)$ for all times greater than 30 months are equal to 1.0 in Eq. 4. For all times less than 30 months, the values for $p_D(t)$ are proportional to the

square root of time. This follows directly from the relationship expressed in Eq. 3. For example, $p_D(25) = \sqrt{25/30}$. Using these definitions, Eq. 4 becomes:

$$\frac{k A \Delta p}{\mu L} = q_1(1) + (q_2 - q_1)(1) + (q_3 - q_2)(1) + (q_4 - q_3)\sqrt{25/30} + (q_5 - q_4)\sqrt{15/30} + (q_6 - q_5)\sqrt{10/30} \quad (5)$$

Notice the left hand side of Eq. 5 is equal to the flow rate if we had linear steady-state flow; thus, we can call this term the equivalent steady-state flow rate, q_{eq} . The right hand side contains a number of terms that cancel each other, so the equation can be simplified as follows:

$$q_{eq} = q_3 + \frac{1}{\sqrt{30}} [(q_4 - q_3)\sqrt{25} + (q_5 - q_4)\sqrt{15} + (q_6 - q_5)\sqrt{10}] \quad (6)$$

Equation 6 gives us a basis for a general formulation for calculating the equivalent flow rate as a function of the lag time.

Because the transient properties of the reservoir are not known, the lag time is not known. Thus, it is necessary to calculate a least-squares fit assuming various lag times, and then choose the lag time which gives the best fit to the data. Thus, it is necessary to calculate the equivalent flow rates at various lag times using transient multipliers as in Eq. 6 above. The calculated equivalent flow rates were based on the **gross** steam rate from the reservoir, calculated from the data in Table 1. These flow rates are listed in Tables 3 and 4 on the following pages for a lag time of 30 months. Notice in Table 3 that production from Unit D has been separated from production in the Unit

A-C, E and F area. In Table 4, production from both Unit D and F have been separated from Units A-C and E. The reasons for these divisions will be clarified later in the report, where we discuss drawdown behavior in various portions of the reservoir.

When we combine the concept of reservoir depletion in a deep boiling zone with the concept of linear flow from that zone to the producing horizon, the reservoir depletion model can be written in the following form:

$$(p/Z)_{top} = (p/Z)_{deep} - \Delta(p/Z)_{flow} \quad (7)$$

where :

$(p/Z)_{top}$ = the p/Z seen at the producing zone; it is less than the value of p/Z within the deep boiling interval due to linear flow from the deep zone to the producing zone.

$(p/Z)_{deep}$ = the value of p/Z at the deep boiling zone; this value drops as the zone depletes.

$\Delta(p/Z)_{flow}$ = the drop in p/Z due to steam flow from the deep zone to the upper producing interval.

Table 3

GROSS EQUIVALENT FLOW RATES
 (Units A-C, E, F together; Unit D separate)
 Equivalent flow rate, q_{eq} , 10^9 lbs./mo.

Months	Gross Rate		t lag = 30 mo	
	Units		Units	
	A-C, E, F	D	A-C, E, F	D
71	0.46	0	0.46	0
77	0.47	0	0.46	0
93	0.66	0	0.60	0
107	0.90	0	0.83	0
117	0.98	0	0.92	0
132	1.17	0	1.11	0
144	1.75	0	1.53	0
154	2.66	0	2.19	0
167	2.64	0	2.53	0
175	2.58	0.31	2.61	0.16
182	2.48	0.62	2.55	0.37
192	2.61	0.75	2.58	0.59
200	2.63	0.79	2.60	0.71
206	2.53	0.74	2.57	0.74
212	2.74	0.64	2.66	0.71
220	2.51	0.55	2.58	0.64
226	2.70	0.68	2.64	0.66
235	2.98	0.68	2.83	0.66
249	2.99	0.71	3.02	0.69

Table 4

GROSS EQUIVALENT FLOW RATES
 (Units A-C, E together; Units D and F separate)
 Equivalent flow rate, q_{eq} , 109 lbs./mo.

Months	Gross Rate			$t_{lag} = 30$ mo.		
	Units A-C, E	Units D	F	Units A-C, E	Units D	F
71	0.46	0	0	0.46	0	0
77	0.47	0	0	0.46	0	0
93	0.66	0	0	0.60	0	0
107	0.90	0	0	0.83	0	0
117	0.98	0	0	0.92	0	0
132	1.17	0	0	1.11	0	0
144	1.75	0	0	1.53	0	0
154	2.66	0	0	2.19	0	0
167	2.64	0	0	2.53	0	0
175	2.58	0.31	0	2.61	0.16	0
182	2.48	0.62	0	2.55	0.37	0
192	2.61	0.75	0	2.58	0.59	0
200	2.63	0.79	0	2.60	0.71	0
206	2.43	0.74	0.10	2.52	0.74	0.046
212	2.61	0.64	0.13	2.58	0.71	0.077
220	2.38	0.55	0.13	2.47	0.64	0.11
226	2.54	0.68	0.16	2.51	0.66	0.13
235	2.76	0.68	0.22	2.64	0.66	0.18
249	2.74	0.71	0.25	2.72	0.69	0.23

The problem now is to define the changes in p/Z as a function of the volume produced and the producing rate. First, let us consider $(p/Z)_{\text{deep}}$. The work by Brigham and Morrow (1977) shows that the value of p/Z in a boiling system is nearly linear with cumulative production, at least for the first 1/3 to 1/2 of the total depletion history. Because some of the condensed water is reinjected in this reservoir and clearly shows signs of evaporation, it seems proper to use only the net cumulative production for this depletion term. With this type of model, the equation is:

$$(p/Z)_{\text{deep}} = A - B G_{p_{\text{net}}} \quad (8)$$

where :

A = the initial p/Z of the deep reservoir system.

B = the constant which defines the depletion rate of the reservoir; a larger B signifies a smaller reservoir.

The next problem was to determine $\Delta(p/Z)$ due to linear flow. This is discussed in the next section.

5. RELATING $\Delta(p/Z)$ TO FLOW RATE

Equation 6 relates the equivalent steady state flow rate to the actual rates; however, this equation was written for liquid flow rather

than steam flow. The correct equation for the equivalent steady state flow of steam is:

$$\int_{p_1}^{p_2} \frac{2pdp}{\mu Z} \Delta m(p) \quad (9)$$

where :

$$m(p) = \int_{p_{sc}}^{p_2} \frac{2pdp}{\mu Z}$$

and C' = an unknown constant inversely proportional to the permeability in the deep fractured zone.

Atkinson and Mannon (1977) have shown that $m(p)$ is almost exactly proportional to p^2 for steam reservoirs. Thus, Eq. 9 can be simplified to:

$$q_{eq} = C'' \Delta(p^2) \quad (10)$$

Note that Eq. 10 relates flow rate to $\Delta(p^2)$, while Eq. 7 requires that the flow rate be related to $\Delta(p/Z)$. There is no theoretical basis whereby these terms can be related; however, it seems reasonable to assume that an empirical power law equation of the following form could be developed:

$$\Delta(p/Z)_{flow} = C' \frac{\Delta(p^2)_{top}^n}{(p/Z)_{top}^m} = C \frac{(q_{eq})^n}{(p/Z)_{top}^m} \quad (11)$$

The reasoning behind Eq. 11 is as follows: For a greater $\Delta(p^2)$, frictional flow effects will be greater. For a greater $(p/Z)_{top}$, frictional flow effects will be smaller, because there will not exist as great a pressure drop between the top and bottom of the reservoir. To test whether this equation form would work, values of $\Delta(p^2)$ and $\Delta(p/Z)$ were calculated for reservoir steam at values of p/Z ranging from 375.0 ($p = 340$ psi) to 738.6 ($p = 600$ psi). This encompassed the entire pressure range of the reservoir history as well as projections for several years into the future. The resulting best fit equation was the following:

$$\Delta(p/Z)_{flow} = C \frac{(q_{eq})^{0.987}}{(p/Z)_{top}^{0.257}} \quad (12)$$

The maximum error of the regression was less than 2.2%.

We could now combine Eqs. 7, 8, and 12 into a working depletion equation:

$$(p/Z)_{top} = A - B G_{p_{net}} - C \frac{(q_e)^{0.987}}{(p/Z)_{top}^{0.257}} \quad (13)$$

This equation is linear, so it can be used in a linear regression formulation to calculate best values for the constants A, B, and C to match the pressure history. However, it was discovered that communication with the deep zone was apparently more tenuous for Unit D

than it was for Units A-C. In other words, a greater pressure drawdown was associated with production from the Unit D area than with production from the Unit A-C area. Therefore, it was necessary to add an additional parameter to Eq. 13 to describe the fractured system in the Unit D area. This final equation had the following form:

$$(p/Z)_{top} = A - B G_{p_{net}} - C \frac{(q_{A-C})^{0.987}}{(p/Z)_{top}^{0.257}} - D \frac{(q_D)^{0.987}}{(p/Z)_{top}^{0.257}} \quad (14)$$

The constant A in the equation is the initial value of p/Z. The second constant is inversely proportional to the size of the system (the reserves). The third constant, C, describes the vertical linear flow behavior of steam in the Unit A-C area, while the final constant, D, describes the flow behavior in the Unit D area. Eq. 14 was found to fit the data very well. Several lag times produced reasonable fits, but Brigham, in other calculations, found that a lag time of 30 months produced the best results. Using only data through the 18th year (the first 15 data points in Table 1), the least squares fit of Eq. 14 for a 30 month lag time was the following:

$$(p/Z)_{top} = 719.2 - 0.2245 G_{p_{net}} - 49.4 \frac{(A-C)^{0.987}}{(p/Z)_{top}^{0.257}} - 424 \frac{(q_D)^{0.987}}{(p/Z)_{top}^{0.257}} \quad (15)$$

Note that in Eq. 15 flow rates from Unit D have been separated from all other units. This is how the data are presented in Table 3.

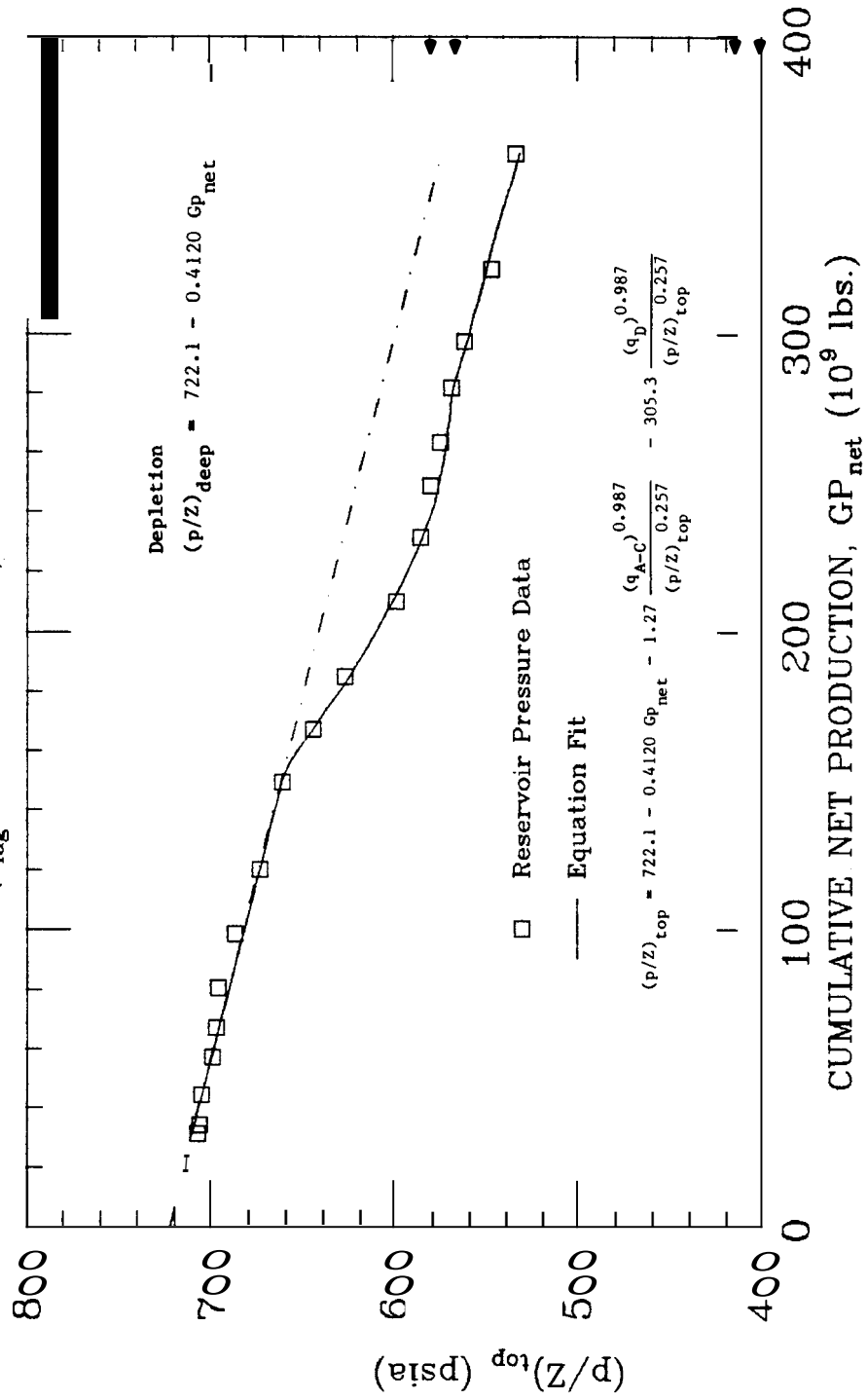
6. CURRENT RESERVOIR HISTORY MATCHING EFFORTS

As new data became available during the course of the study, we were able to determine whether Eq. 15 was accurately predicting the reservoir performance. Using all 19 data points in Table 1, the best fit equation of the form in Eq. 14 for a lag time of 30 months was the following:

$$\begin{aligned}
 (p/Z)_{\text{top}} = & 722.1 - 0.4120 Gp_{\text{net}} - 1.27 \frac{(q_{\text{A-C}})^{0.987}}{(p/Z)_{\text{top}}^{0.257}} \\
 & - 305.3 \frac{(q_{\text{D}})^{0.987}}{(p/Z)_{\text{top}}^{0.257}} \quad (16)
 \end{aligned}$$

The above equation suggests that frictional flow of steam in the Unit A-C area had a minimal effect on the pressure drop between the deep boiling zone and the producing horizon. Notice, in particular, the significantly decreased value of the constant C compared with that in Eq. 15. This constant is directly proportional to the amount of drawdown due to frictional flow in the Unit A-C area. The value of C in Eq. 16 suggests that this frictional flow drawdown was insignificant. This can be seen more clearly in Fig. 4. Over 76% of the total pressure drop is due to depletion, and this is a result of the small value of the constant C in Eq. 16 and of the rather large value of the constant B in Eq. 16 compared with its value in Eq. 15. These results are in direct contradiction to the model, because the model is based on the concept of a deep boiling zone, above which frictional flow effects must occur as

FIGURE 4
 PRESSURE-PRODUCTION HISTORY MATCH
 ($t_{lag} = 30$ months)



the steam rises to the producing zone. It is also in contradiction to the results using the first 15 data points. For these reasons, the Eq. 16 fit appears to be invalid.

To produce more reasonable values for the frictional flow constants, C and D, greater lag times were used. A lag time of 70 months produced a regression fit similar to Eq. 15. However, a very interesting question arises at this point. Is it reasonable to develop a model in which lag times have to be changed to yield an acceptable match? This is a crucial question for which there is no definite answer. The transient properties of the reservoir are not known, and therefore the lag time is not known. In addition, the time matches that we have used are simply not that diagnostic to assume that one is more valid than another. A 70 month lag time may describe the transient phenomena more precisely than a 30 month lag time. We don't know which is correct.

Predictions of future performance are often quite respectable when the history match is good, even though the model might not be a correct representation of the reservoir. However, these predictions would be even more acceptable if the same lag time produced an accurate match as new data became available and if the constants in the empirical equation did not change significantly as time goes on. In other words, can Brigham's model be modified so that a 30 month lag time would produce a reasonable history match for all 19 data points? If so, the model would then consistently describe the transient properties of the pressure cell. The answer to this question will be developed in the next section.

7. ANALYSIS OF FRICTIONAL FLOW CONSTANTS

As previously mentioned in this study, the $\Delta(p/z)_{\text{flow}}$ constants, C and D, of Eq. 15 describe the reservoir frictional flow characteristics of the Unit A-C and D areas respectively. As production of steam continues and more data become available, these frictional flow constants should not change, because they are proportional to certain reservoir flow properties, such as permeability, which are constant. Therefore, a sensitivity analysis was performed on the pressure-production data to determine whether C varied with time. Starting with the first nine data points, and using a lag time of 30 months, a multiple linear regression was run to produce a fit in the form of Eq. 14. The constant, C, was tabulated, and then an additional data point was included in the regression. The process was repeated until data through 212 months were included. The results showing the various values of C are listed in Table 5:

Table 5

SENSITIVITY OF FRICTIONAL FLOW CONSTANT, C
($t_{\text{lag}} = 30$ months)

<u>Months</u>	<u># Data Points</u>	<u>C</u>
167	9	123.1
175	10	123.1
182	11	125.4
192	12	122.6
200	13	118.4
206	14	92.4
212	15	49.4
249	19	1.3

The values of C listed above remain approximately constant with time until approximately 200 months. From that point on, C declines with time until 249 months, when it equals the unrealistic value of 1.3, seen in Eq. 16. A steady value of approximately 123 describes the

linear flow behavior of Units A-C for a significant period of time. Therefore, it seems logical to assume that lag times should not have to be changed, as time progresses, to produce a history match with reasonable frictional flow constants. Table 3 shows that the most accurate value for C is about 123. Thus, the next step in the modification of the model was to determine what other phenomena could have been causing C to decline from this value subsequent to 200 months, and then to produce a history match with more reasonable values for both C and D.

8. ANALYSIS OF UNIT F BEHAVIOR

In a preliminary analysis of these data, Brigham determined that a more tenuous communication with the deep zone was responsible for higher drawdown behavior in the Unit D area. Separating the flow rates of Units A-C from the rate in Unit D, and using different constants on the individual flow and pressure drop terms produced an excellent match. We discovered that Unit F was also causing a higher pressure drop. Therefore, the flow rates of Unit F were separated from those of Units A-C and D, and a third flow and pressure drop term was added to the model. Note that flow rate data in Table 4 are presented accordingly. The resulting equation form is shown on the following page.

$$\begin{aligned}
 (p/Z)_{\text{top}} = & A - B G p_{\text{net}} - C \frac{(q_{\text{A-C}})^{0.987}}{(p/Z)_{\text{top}}^{0.257}} - D \frac{(q_{\text{D}})^{0.987}}{(p/Z)_{\text{top}}^{0.257}} \\
 & - E \frac{(q_{\text{F}})^{0.987}}{(p/Z)_{\text{top}}^{0.257}}
 \end{aligned} \tag{17}$$

This equation now has an additional constant, E, and the form of the equation produced an excellent match as will be seen later.

It might be argued that a least squares fit of 19 data points using Eq. 17 is statistically unsound, since an equation of 4 independent variables would closely match any set of 19 data points. However, the purpose of Eq. 17 is to describe the differing flow mechanisms of the reservoir. The above equation form produced values for C and D that were very similar to the previous values. Thus, the model can be used without the need to change the lag time to produce a valid match.

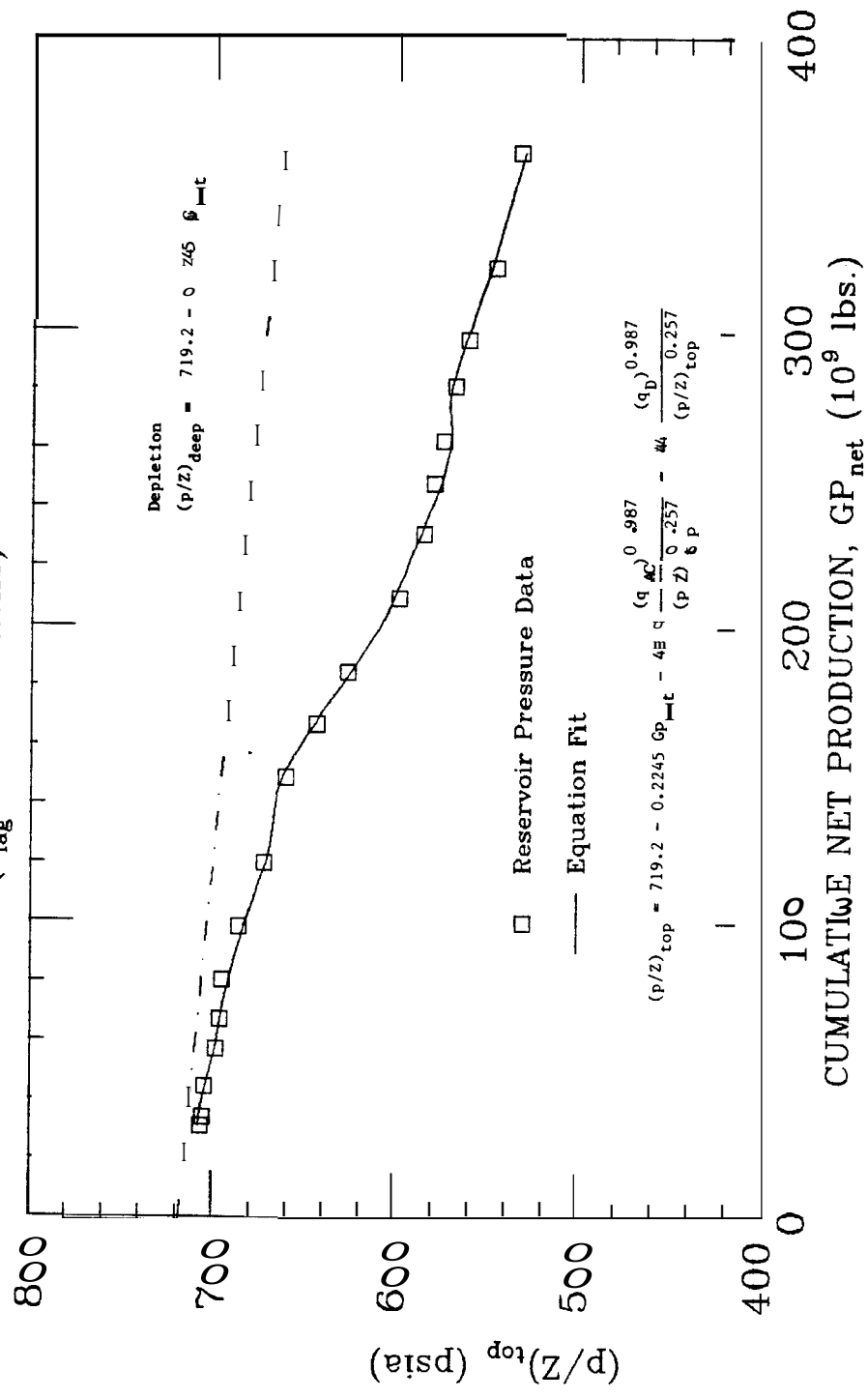
9. RESERVOIR PRESSURE MATCH AND EXTRAPOLATION

A lag time of 30 months (Fig. 5) was used for Eq. 17 so that the frictional flow constants could be compared with those in Eq. 15. Note in Table 4 that equivalent flow rates for Unit F began at 206 months. This is a slight overlap from the previously discussed history match. The rates had been small enough so that the effects of Unit F would not have been felt by the reservoir at that time.

The least squares fit to the data using Eq. 17 with a lag time of 30 months is the following:

$$\begin{aligned}
 (p/Z)_{top} &= 718.5 - 0.1544 Gp_{net} - 71.2 \frac{(q_{A-C})^{0.987}}{(p/Z)_{top}^{0.257}} \\
 &= 436.7 \frac{(q_D)^{0.987}}{(p/Z)_{top}^{0.257}} - 717.4 \frac{(q_F)^{0.987}}{(p/Z)_{top}^{0.257}} \quad (18)
 \end{aligned}$$

FIGURE 5
 PRESSURE-PRODUCTION HISTORY MATCH
 ($t_{lag} = 30$ months)



The frictional flow constant, C, describing flow behavior in Units A-C, is equal to 71.2 in Eq. 18. Although this is less than 123, the value we had hoped to achieve, 71.2 is much more reasonable than a value of 1.3 seen in Eq. 17. In addition, 71.2 is closer to the value of C in Eq. 15, which was the original regression fit of data to 212 months. The same comparisons pertain to the frictional flow constant, D, in Eq. 20. For example, 436.7 in Eq. 18 compares to 424.0 in Eq. 15. Therefore, we have modified Brigham's model to include Unit F behavior and have produced a reasonable match without changing the assumptions concerning the transient properties (the lag time) of the reservoir.

Let us now turn to prediction of future performance of the reservoir. In order to extrapolate the data, it was necessary to estimate the future reservoir production rates subsequent to 249 months. It was also necessary to predict whether new power plants would act like Units A-C, Unit D, or Unit F in their linear flow behavior, and what portion of the new plants' production would come from this pressure cell. Table 6 below summarizes these estimates:

Table 6

SUMMARY OF PROJECTED NEW UNIT BEHAVIOR

<u>Unit Letter</u>	<u>Starting Month</u>	<u>Unit Size</u>	<u>Gross Production Rate from Study Area (10⁹ lbs./mo.)</u>	<u>Equivalent Unit Behavior</u>
E	On Line	Large	0.49	A-C
F	On Line	Small	0.21	F
G	305	Small	0.35	A-C, F
H	269	Large	0.70	D

Next, it was necessary to calculate net cumulative production and equivalent flow rates for the future based on the data from Table 4. A reinjection rate of 25% of the gross production has been assumed for the

net cumulative production figures. These projections are listed in Table 7 for a lag time of 30 months. In Table 7, the column labelled "Units A-C" includes Units A, B, C, E, and half of Unit G. The column labelled "Unit D" includes Unit D and Unit H. The column labelled "Unit F" includes Unit F and half of Unit G.

Using the data from Table 7, it is possible to project p/Z decline into the future using Eq. 18. However, such predictions do not take into account the deliverability of the reservoir. Certainly, it is not possible to produce at a constant rate indefinitely, unless there is 100% recharge in the system. At some point in the future, the reservoir pressure will have declined such that the flow rate must start declining as well. Drilling more wells will help for a period of time, but according to this model, the problem of deliverability is a reservoir problem.

In the following section, the deliverability problem is addressed in full. The deliverability equations are then combined with Eq. 18 to predict both p/Z decline and flow rate decline for the reservoir.

10. DELIVERABILITY AND FUTURE PRODUCING RATES

In general, for gas flow from a reservoir, it is possible to calculate flow rate based on a version of the Forchheimer equation), known as the universal deliverability equation. The development of this equation proceeds as follows.

Table 7

FUTURE PRODUCTION AND DESIRED EQUIVALENT FLOW RATES

Year	Net Cumul. Prod. (10 ⁹ lbs.)	Units A-C; q_{eq} $t_{lag} = 30$	Unit D; q_{eq} $t = 30$	Unit F; q_{eq} $t = 30$
23.5	435.7	2.80	1.01	0.21
24.0	455.5	2.80	1.14	0.21
24.5	475.4	2.80	1.24	0.21
25.0	495.2	2.80	1.33	0.21
25.5	515.1	2.80	1.40	0.21
26.0	534.9	2.80	1.40	0.21
26.5	556.3	2.88	1.40	0.29
27.0	577.8	2.91	1.40	0.32
27.5	599.2	2.94	1.40	0.35
28.0	620.6	2.96	1.40	0.37
28.5	642.0	2.97	1.40	0.38
29.0	663.4	2.975	1.400	0.385
29.5	684.9	2.975	1.400	0.385
30.0	706.3	2.975	1.400	0.385
30.5	727.7	2.975	1.400	0.385
31.0	749.1	2.975	1.400	0.385

At high **flow** rates, in addition to the viscous force represented by Darcy's equation, there also exists an inertial force caused by convective acceleration of the fluid molecules passing through pore spaces, as described by Geertsma (1974). The appropriate equation describing these conditions is the Forchheimer equation:

$$-\frac{dp}{dx} = \frac{\mu}{k} v + \beta \rho v^2 \quad (19)$$

as the coefficient of inertial resistance. The density, ρ , and the velocity, v , are each functions of pressure. In order to perform the

$$-\rho \frac{dp}{dx} = \frac{\mu}{k} (\rho v) + \beta (\rho v)^2 \quad (20)$$

The term ρv is the mass rate of flow and is therefore independent of pressure. By using the real gas laws, we can express ρv in the following way:

$$\rho v = \frac{q_{sc} p_{sc} M_w}{A T_{sc} R} \quad (21)$$

where :

sc = standard conditions.

Substitution of the mass flow rate expression (Eq. 21) into Eq. 20 produces the desired universal deliverability equation:

$$\frac{M_w p}{Z R T} \frac{dp}{dx} = \frac{\mu}{k} \frac{p_{sc} M_w}{T_{sc} R} \frac{q_{sc}}{A} + \beta \frac{p_{sc} M_w}{T_{sc} R} \frac{q_{sc}^2}{A} \quad (22)$$

Separating variables, integrating and rearranging the above equation results in our working deliverability equation:

$$p_2^2 - p_1^2 = aq + bq^2 \quad (23)$$

where :

q = the producing rate

a & b = unknown constants which include μ/k , β , and the real gas law terms.

We are now able to use Eq. 23 to develop a reservoir, well, and surface flowline model, which can then be combined with the depletion equations developed earlier. In essence, Eq. 23 can be applied to three different flow configurations:

- 1) Flow from the reservoir to the well,
- 2) Flow from the bottom of the well to the wellhead, and
- 3) Flow from the wellhead to the power plant.

Each of these configurations will produce different values for the unknown constants a & b in the deliverability equation. However, the three resulting equations can be added to produce one equation describing flow from the reservoir to the inlet of the power plant. The resulting equation has the following form:

$$\bar{p}^2 - p_{inlet}^2 = a'q + b'q^2 \quad (24)$$

where :

- \bar{p} = the average producing zone pressure (psi)
- p_{inlet} = the pressure at the inlet to the power plant (psi)
- q = the producing rate (Mlb./mo./well)
- a' & b' = unknown constants

The constant, a' , expresses the Darcy resistance to flow in the reservoir. The constant, b' , expresses the sum of non-Darcy flow in the reservoir plus flowing friction within the well and surface flow line.

The historical production rate data for the reservoir were tested against this equation. This was first done on a Unit by Unit basis,, which produced excellent results. Let us look at Eq. 24 in more detail. If we divide both sides of the equation by the flow rate, q , we produce an equation for a straight line as follows:

$$\Delta p^2/q = a' + b'q \quad (25)$$

Therefore, graphing $\Delta(p)^2/q$ versus q should produce a straight line whose slope and intercept yield the desired values of the unknown constants, a' & b' . Various values of q and $\Delta(p)^2/q$ for specific Unit areas are listed in Table 8, while the corresponding values for all Units combined are listed in Table 9.

TABLE 8

Table 8

DELIVERABILITY DATA

YEAR	Unit A			Unit B			Unit C			Unit D		
	\bar{p}	P_{inlet}	$q \Delta p^2/q$	\bar{p}	P_{inlet}	$q \Delta p^2/q$	\bar{p}	P_{inlet}	$q \Delta p^2/q$	\bar{p}	P_{inlet}	$q \Delta p^2/q$
12	482	70	1188.9	191.3	-	-	-	-	-	-	-	-
13	452	70	1047.6	190.3	500	105	2002.0	119.4	548	105	2140.7	135.1
14	431	70	948.6	190.7	469	105	1778.8	117.5	534	105	1974.2	138.9
15	407	70	854.4	188.1	437	105	1655.4	108.7	501	105	1878.9	127.7
16	380	70	731.9	190.6	410	105	1497.6	104.9	464	105	1626.7	125.6
17	354	70	674.7	178.5	381	105	1369.7	97.9	435	105	1485.7	119.9
18	336	70	600.6	179.8	356	105	1239.8	93.3	415	105	1285.2	125.4
19	324	70	584.1	171.3	342	105	1237.4	85.6	403	105	1297.2	116.7
20	317	70	733.3	130.4	336	105	1139.1	89.4	394	105	1281.2	112.6
21	-	-	-	-	-	-	-	-	-	-	-	-

p=(psia)

q=(Mlb/day/well)

Table 9

DELIVERABILITY DATA
(ALL UNITS COMBINED)

Year	P_{inlet}	q	$\Delta p^2/q$
13	560	105	1772.1
14	546	105	1616.9
15	527	105	1660.2
16	500	105	1502.0
17	483	105	1363.3
18	471	105	1203.4
19	461	105	1166.7
20	449	105	1119.7

p = (psia).

q = (Mlb/day/well).

The values listed in Tables 8 and 9 are shown graphically in Figs. 6, 7, 8, 9, and 10. Let us look at these figures in more detail. Figs. 6, 7, 8, and 9 show excellent results for a straight line match. Figure 7, which depicts deliverability in the Unit B area, reveals the steepest slope for the straight line match. This is a result of an increased value of b' in Eq. 25, which shows that non-Darcy flow is more significant in this area. Figure 9 reveals a slope equal to zero for Unit D. Apparently, all flow can be represented by Darcy flow in this area, since the non-Darcy component, b' , is equal to zero. In each of these figures it is evident that a' and b' assume different values. In other words, the deliverability is different for each Unit area of the reservoir. A question then arises. How can we relate these individual deliverabilities to the system as a whole? In addition, the reservoir pressure is interdependent between Eq. 18 and Eq. 24. Thus, the

FIGURE 6
 DELIVERABILITY ANALYSIS
 (Unit A)

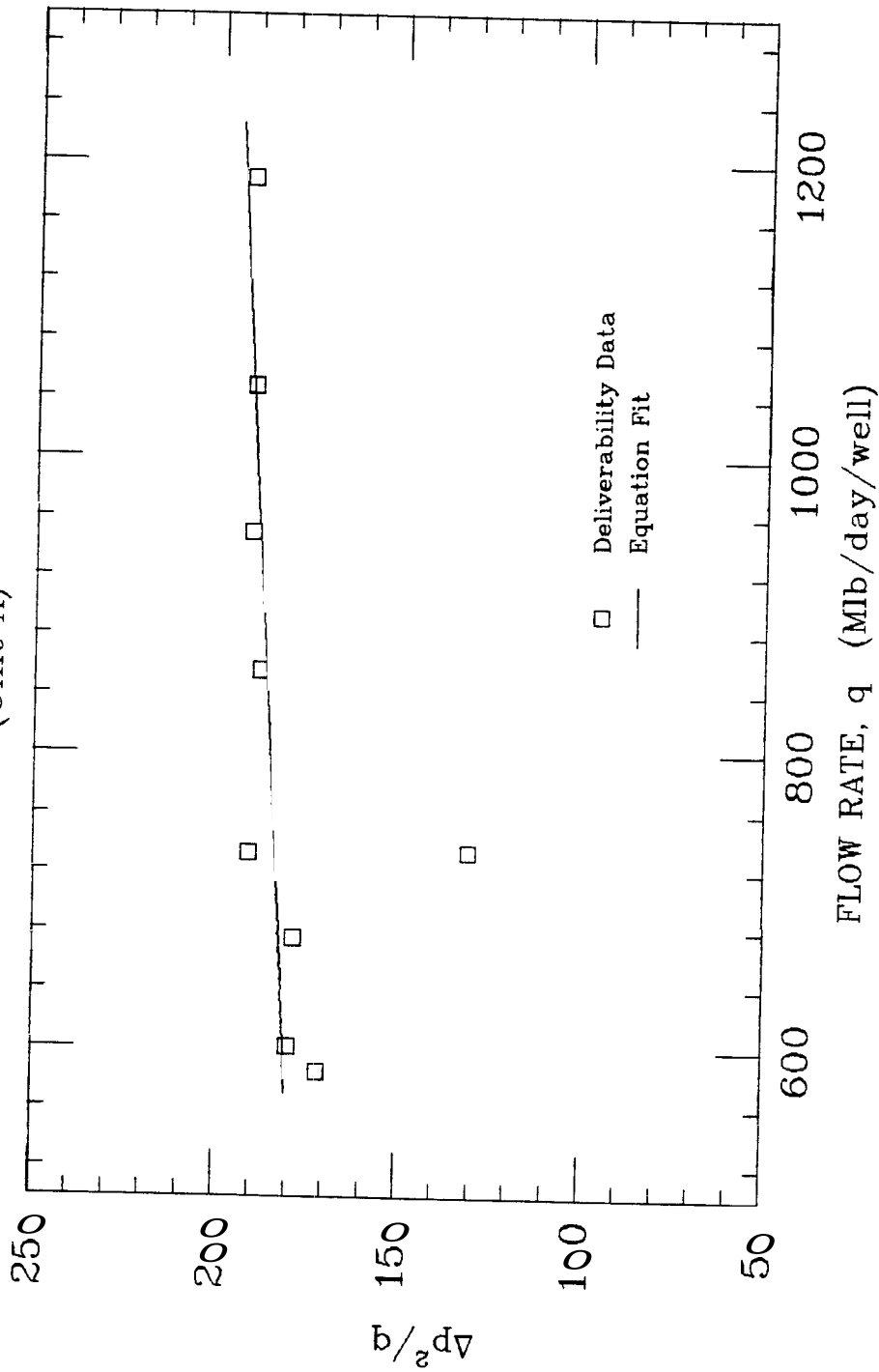


FIGURE 7
 DELIVERABILITY ANALYSIS
 (Unit B)

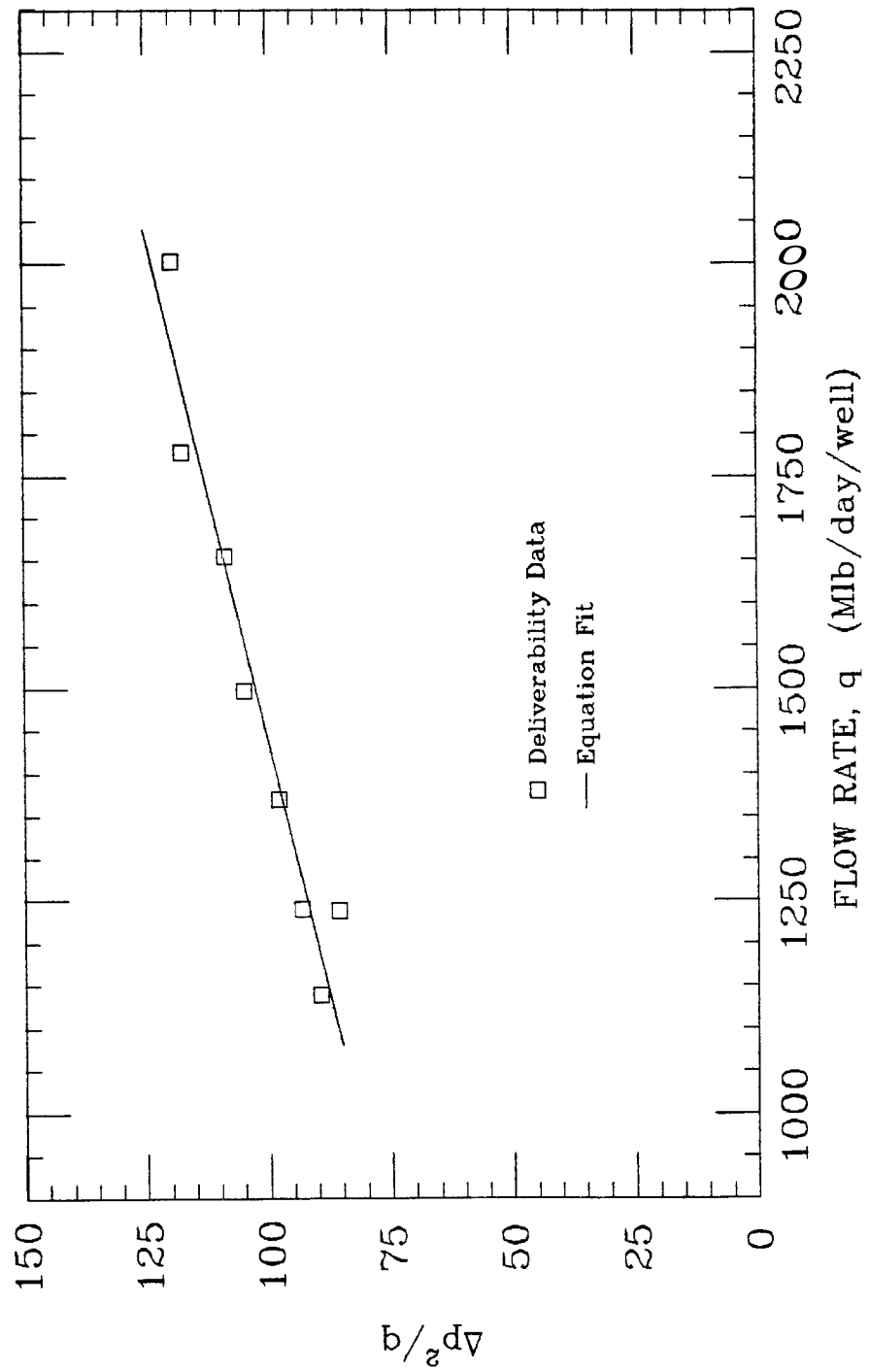


FIGURE 8
 DELIVERABILITY ANALYSIS
 (Unit C)

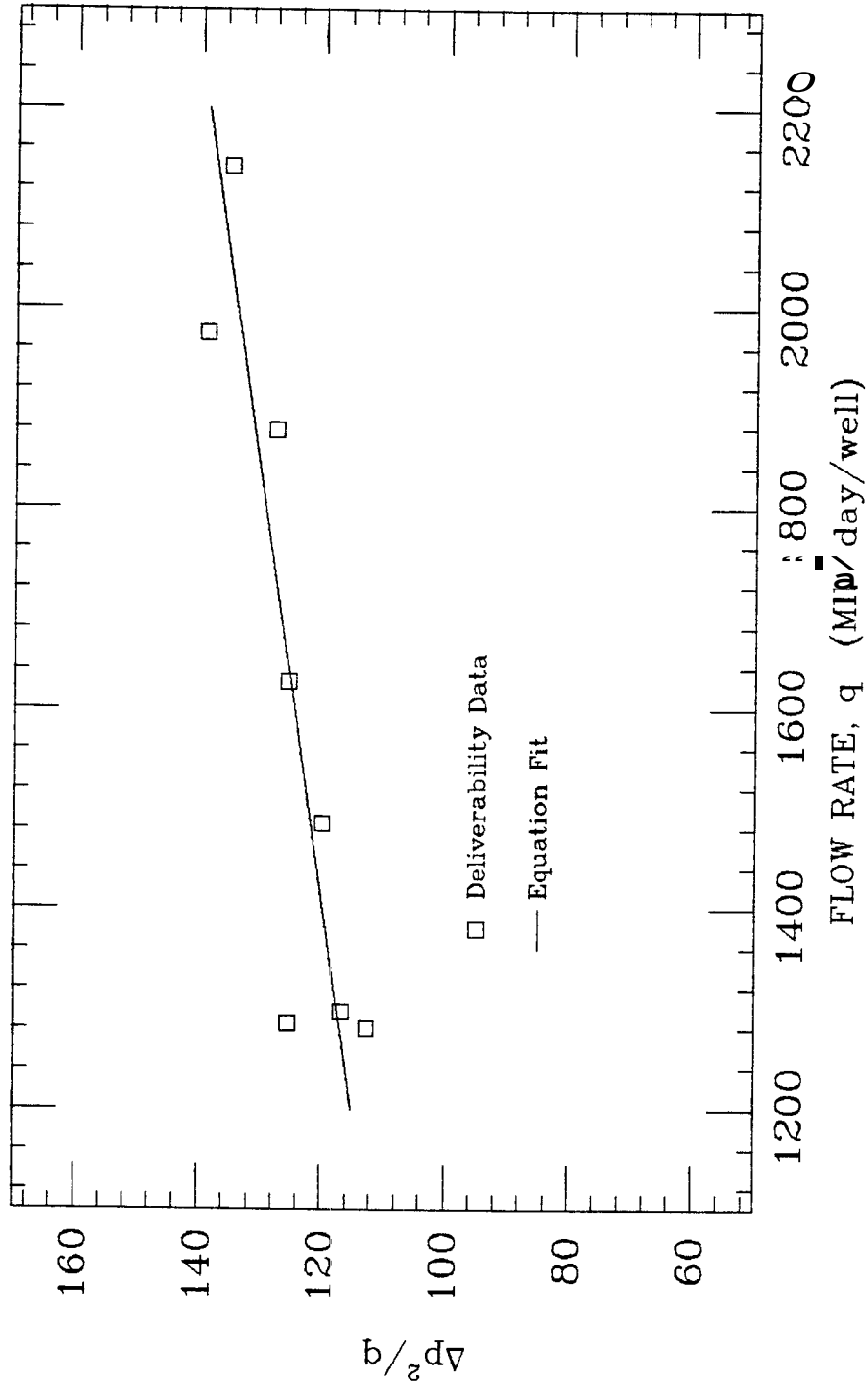


FIGURE 9
 DELIVERABILITY ANALYSIS
 (Unit D)

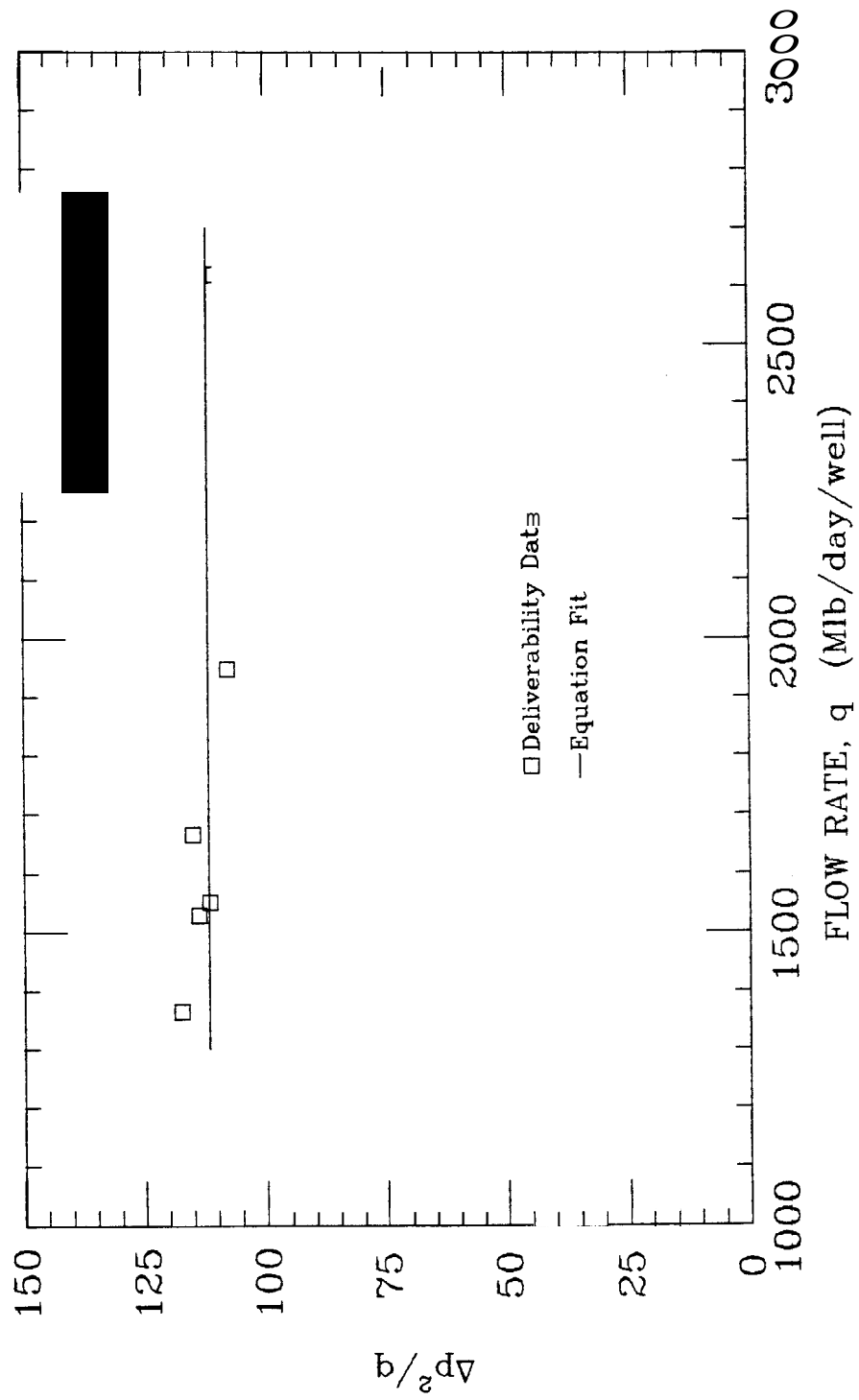
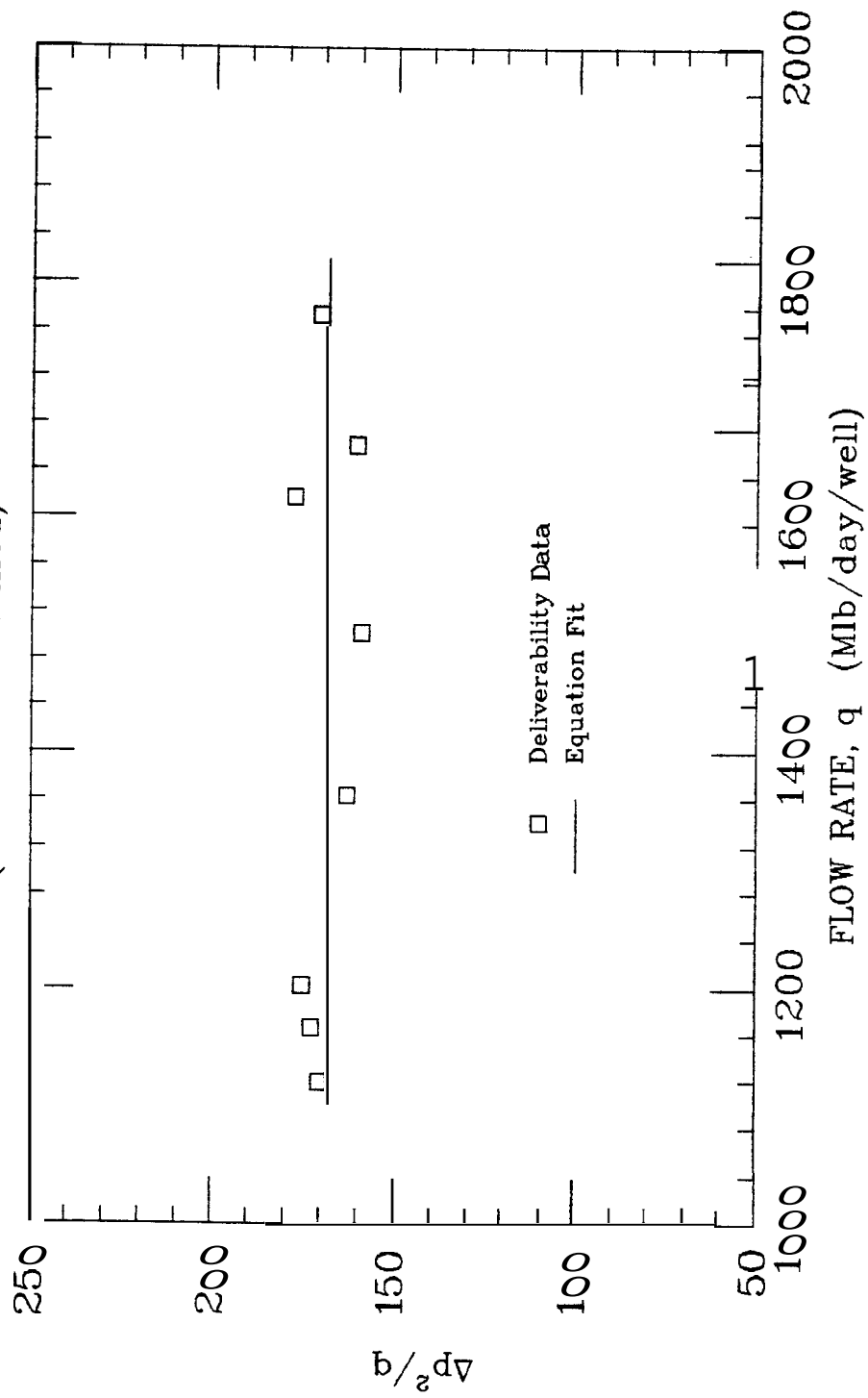


FIGURE 10
 DELIVERABILITY ANALYSIS
 (All Units Combined)



deliverability of the entire system must be represented in terms of the average reservoir pressure seen in Eq. 18, which is higher than the individual average reservoir pressures seen in the vicinity of the wells (Eq. 24).

To answer these questions and accomplish these tasks, the individual flow rate data in Table 8 have been combined to produce an overall flow rate per well for the entire reservoir, and the average reservoir pressures have been used rather than the individual pressures. These values are listed in Table 9. The average pressures seen in Table 9 are higher than those seen in Table 8, as discussed above. The data were graphed in Fig. 10 to show the overall deliverability of the reservoir.

An important point here is that the pressure in the vicinity of the wells reflects the true deliverability of the system, while in Fig. 10 we are dealing only with the average reservoir pressure. By using average reservoir pressure instead of pressure in the vicinity of the wells, higher values for a' and b' are calculated, resulting in what appears to be a lower deliverability. Actually, using this technique, both the true deliverability and the true pressure in the vicinity of the wells have been incorporated into the model.

Notice in Fig. 10 that a straight line of zero slope matches the data reasonably well. We found that the reservoir production rate could be matched with a maximum error of 6.0% using the following equation:

$$\frac{p}{p} - p_{inlet}^2 = 5.54 q \quad (26)$$

where :

$$q = \text{flow rate (Mlb./mo./well)}$$

As Fig. 10 indicates, the non-Darcy component, b' , was found to be negligible. This does not mean that the non-Darcy term is negligible for this reservoir. This is an artifact of the reservoir pressure averaging process used to fit the equation.

We can now project flow rates and pressures into the future, assuming that plant inlet pressures remain constant at 105 psi. These projections require a trial and error calculation, because both flow rate and pressure are interdependent in Eqs. 18 and 26. Rapid convergence to the answers occurred in 2 to 4 iterations. The trial and error method that we used sets both the pressure and flow rate at the new level of iteration equal to the values at the old level of iteration. Eq. 18 then produced a new value for p/Z , and Eq. 216 produced a new value for q . These new values were then used to continue the iteration in Eq. 18 until convergence was achieved.

Inherent in these projections of flow rate and pressure is the underlying assumption of future drilling. We have assumed three scenarios in our predictions: the future deliverability will equal 2.0, 2.5, and 3.0 times the current deliverability of the reservoir. However, fewer than 2.0 times the current number of wells will be needed to produce twice the current deliverability of the reservoir, because newer wells will be drilled in higher pressure areas and will therefore have better deliverability than older wells.

The flow rates were projected for 32 years through the year 55, using the lag time equation developed earlier in this report: Eq. 18. These projections are listed in Table 10, where both production rate and pressure are shown. The gross flow rate projections are graphed in Fig. 11.

An important point to notice is that there is not a significant difference between the three different assumptions of future drilling. The three curves in Fig. 11, representing 2.0, 2.5, and 3.0 times the current deliverability of the reservoir are each separated by only two to three years. This emphasizes the fact that drilling new wells can only temporarily relieve the problem of deliverability.

Projections of future p/Z decline are presented in Fig. 12. The solid line is $(p/Z)_{top}$ and the dashed line is $(p/Z)_{deep}$. In Fig. 12 the pressure begins to drop rapidly in the year 23 ($G_{p_{net}} = 415.8 \times 10^9$ lbs./mo.) after Unit H goes on production. This is because Unit H was assumed to have the more tenuous connection with the deep boiling zone. In Fig. 12 this is Labeled "Unit D" since Unit H is assumed to

Table 10

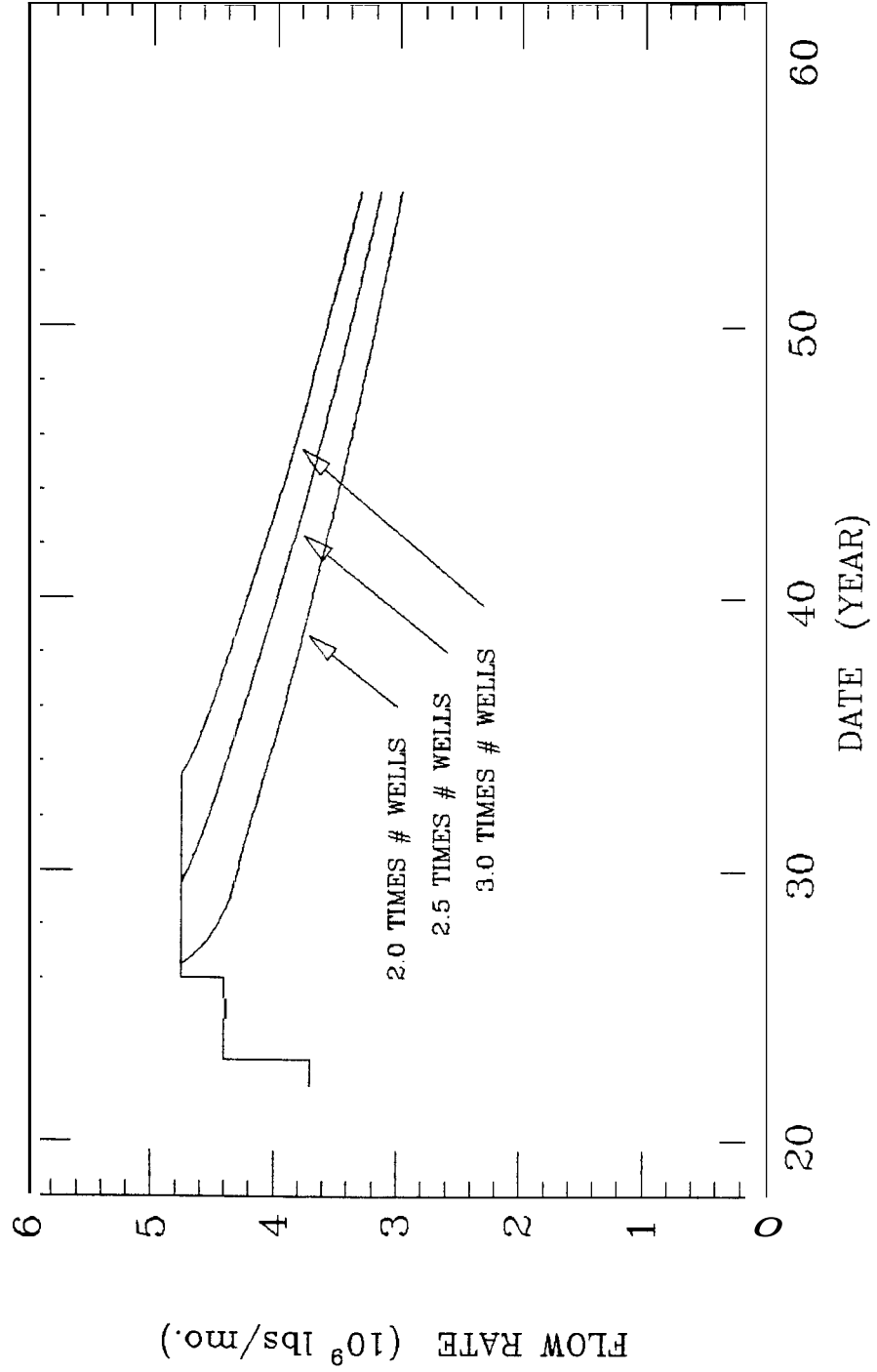
PROJECTIONS OF GROSS FLOW RATE (10^9 lbs./mo.) & PRESSURE (psia)
 (ASSUMES 2.5 TIMES THE CURRENT DELIVERABILITY OF THE RESERVOIR)

t _{lag} = 30 months			
Year	G _{p,net} (10^9 lbs.)	q	p/Z
23.0	415.8	3.71	521.5
24.0	455.5	4.41	474.0
25.0	495.2	4.41	449.0
26.0	534.9	4.41	434.6
27.0	577.8	4.76	405.7
28.0	620.6	4.76	388.8
29.0	663.4	4.76	377.2
30.0	706.1	4.71	371.0
31.0	747.9	4.61	367.1
32.0	789.0	4.53	364.2
33.0	829.4	4.46	361.3
34.0	869.2	4.39	358.4
35.0	908.3	4.32	355.5
36.0	946.8	4.25	352.7
37.0	984.7	4.18	349.8
38.0	1022.0	4.11	347.1
39.0	1058.6	4.05	344.4
40.0	1094.7	3.98	341.7
41.0	1130.2	3.92	339.0
42.0*	1165.2	3.86	336.4

*

For projections to the year 55, see Fig. 11.

FIGURE 11
PROJECTED FLOW RATES ($t_{lag} = 30$ months)



act like Unit D. Another sudden drop in pressure can be seen, beginning in the year 26 ($G_{p_{net}} = 534.9 * 10^9$ lbs./mo.). This is due to production in the Unit G area. Unit G was assumed to behave in a manner similar to Unit F, which was also experiencing a rapid pressure decline. After these rapid drops, the pressure tends to level off again. Then, the pressure decline almost flattens completely at about 370 psia in Fig. 12. This flattened portion of the $(p/Z)_{top}$ curve corresponds to the period of flow rate decline seen in Fig. 11. During this time period, the pressure drawdown due to frictional flow declines as the flow rate declines. Note that after the beginning of flow rate decline, the $(p/Z)_{top}$ and $(p/Z)_{deep}$ curves begin to converge. The separation between the two lines determines the amount of drawdown due to friction.

11. CONCLUSIONS

The reservoir pressure and production data used herein indicate that depletion is occurring in this reservoir. A reasonable assumption of the flow behavior is that there exists a zone of boiling water deep in the reservoir, which supplies steam to the producing horizon where the wells are completed. The pressure drop seen at this producing zone is a combination of depletion of the boiling water and frictional flow effects. The frictional flow drawdown is an additional transient pressure drop due to frictional losses as the steam rises through relatively tight vertical fractures.

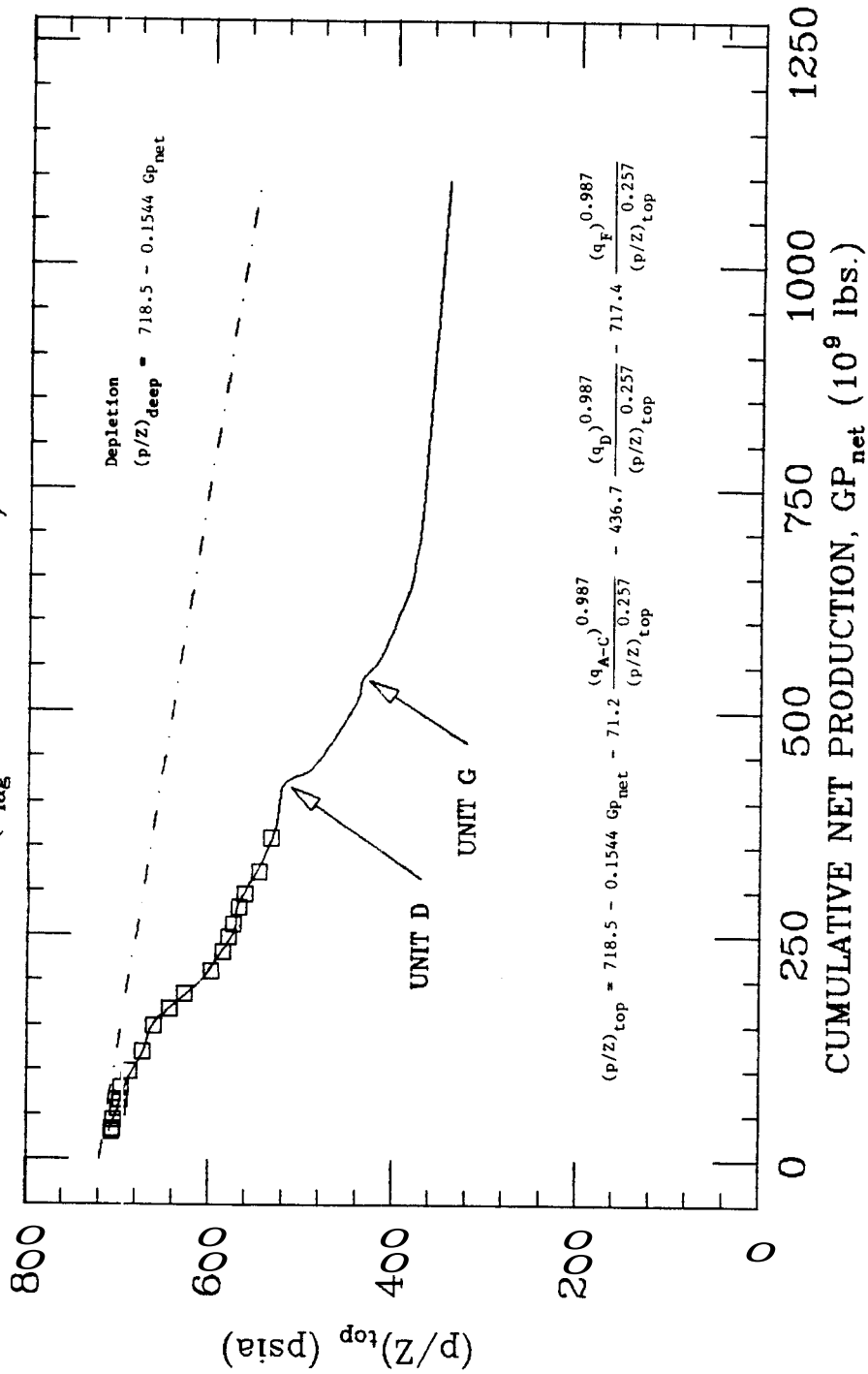
Using the above concepts, we have successfully developed a lumped parameter model describing pressure drawdown in the reservoir. Depletion of the boiling water zone is assumed to fit linearly with p/Z . The transient linear vertical flow is calculated using a lag time

concept to change transient flow into equivalent steady state flow. The lag time is unknown, but a lag time of 30 months has produced a reasonable fit. Various areas within the system have experienced different drawdown behavior, and therefore, the flow rates from these areas were separated from the total flow rate and were then incorporated into separate flow and pressure drop parameters.

The deliverability problem described by these example data is a reservoir problem, and a sustained flow rate can only be maintained until approximately the 30th year. However, subsequent to that time, the flow rate decline will be gradual, in the neighborhood of two percent per year. This is quite similar to the behavior of several geothermal reservoirs.

Many people feel there is considerable "perched" and adsorbed liquid water in inaccessible areas within the producing horizon. As the pressure drops, this "perched" water could boil and the resulting steam would then flow toward the highly permeable channels connected to the wells. Presumably, the flow connection between the perched water and the permeable channels is tenuous. In other words, we are describing a two-porosity system. An important point is that the reservoir model developed herein fits this physical picture equally well. The resulting equations would be identical.

FIGURE 12
 PROJECTED P/Z DECLINE
 ($t_{lag} = 30$ months)



NOMENCLATURE

English

b = linear reservoir width, ft

c_t = total compressibility, psi^{-1}

$F(t_D)$ = dimensionless t_D function

$G_{p_{\text{net}}}$ = net cumulative steam production, 10^9 lbs

h = linear reservoir thickness, ft

k = permeability, md

M_w = molecular weight, lb/lb-mole

p = pressure, psi

p_D = dimensionless pressure

q = production rate, 10^9 lbs/mo

q_{eq} = equivalent steady-state production rate, 10^9 lbs/mo

R = universal gas constant

t = time, months

t_D = dimensionless time

t_{lag} = lag time, months

v = velocity, ft/sec

x = spatial coordinate in x-direction

Z = gas deviation factor

Greek

β = turbulent coefficient for non-Darcy flow

μ = viscosity, cp

ϕ = porosity

ρ = density, lb_m/ft^3

Subscripts

A-C = Units A, B, and C

D = Unit D

D = dimensionless

F = Unit F

eq = equivalent

t = total

REFERENCES

- Brigham, W. E., and Morrow, W. B.: "P/Z Behavior for Geothermal Steam Reservoirs," Soc. Pet. Engr. Jour., Vol. 17, No. 6 (Dec. 1977), pp. 407-412.
- Brigham, W. E., and Neri, G.: "Preliminary Results on a Depletion Model for the Gabbro Zone (Northern Part of Larderello Field)," Transactions, Stanford Geothermal Workshop, Dec. 1979.
- Geertsma, J.: "Estimating the Coefficient of Inertial Resistance in Fluid Flow Through Porous Media," Soc. Pet. Engr. Jour., October 1974, pp. 445-450.
- Keenan, J. H., Keyes, F. G., Hill, P. G., and Moore, J. G.: "Steam Tables (English Units)," John Wiley & Sons, Inc., 1969.
- Mannon, L. S., and Atkinson, P. G.: "The Real Gas Pseudo-Pressure for Geothermal Steam-Summary Report," Proceedings 3rd Workshop, Geothermal Reservoir Engineering, SGP TR-25, Stanford, Ca., Dec. 14-16, 1977, pp. 29-35.
- Miller, F. G.: "Theory of Unsteady-State Influx of Water in Linear Reservoirs," Journal Institute of Petroleum (Nov., 1962) 48,365.
- Nabor, G. W., and Barham, R. H.: "Linear Aquifer Behavior," Jour. Pet. Tech. (May, 1964), Trans. AIME Vol. 231, pp. 561-563.

APPENDIX

The following pages contain a listing of the computer program which was written to make the flow rate and pressure projections in this report. The program is well documented for the user. Essentially, the program contains two parts. The first part employs the reserves model and the second part employs the deliverability model. The trial and error calculation of flow rate is the main algorithm in the program. A listing of a sample run is also included.

```

1. //SIM JOB
2. // EXEC CATFIV
3. //GO.SYSIN DD *
4. $WATFIV
5. C
6. C
7. C
8. C
9. C
10. C THIS PROGRAM IS DESIGNED TO PROJECT FUTURE PRODUCTION,
11. C PRESSURE, AND FLOW RATES OF A GEOTHERMAL RESERVOIR.
12. C THE PROGRAM COMBINES THE
13. C 3-PARAMETER MODEL, WHICH PREDICTS RESERVES, WITH A
14. C DELIVERABILITY MODEL. THESE MODELS HAVE BEEN DISCUSSED
15. C IN DETAIL IN THE ACCOMPANYING REPORT. THE PROGRAM HAS BEEN
16. C WELL DOCUMENTED SO THAT THE USER, UNFAMILIAR WITH THE
17. C DEVELOPMENT OF THE EQUATIONS, CAN MODIFY THE APPROPRIATE
18. C VARIABLES TO UPDATE PROJECTIONS AS NEW PRESSURE-PRODUCTION
19. C DATA BECOME AVAILABLE.
20. C
21. C
22. C THE FOLLOWING MODIFICATIONS SHOULD BE MADE AT THE
23. C STAY? OF EACH RUN:
24. C
25. C
26. C 1) THE VARIABLE 'TEST' DETERMINES WHETHER THE
27. C DELIVERABILITY PART OF THE MODEL IS INCLUDED IN
28. C PROJECTIONS. FOR 'TEST' = 0.0, THE DELIVERABILITY
29. C PART IS NOT INCLUDED. FOR 'TEST' = 1.3, THE
30. C DELIVERABILITY PART IS INCLUDED. NORMALLY, 'TEST'
31. C SHOULD EQUAL 1.0. DO NOT CONFUSE THE VARIABLE
32. C 'TEST' IN THE MAIN PROGRAM WITH THE VARIABLE 'TEST'
33. C IN THE SUBPROGRAMS.
34. C
35. C 2) CHANGE THE VARIABLES A, E, C, D, AND Z FOR THE
36. C APPROPRIATE LAG TIME AND RESERVES MODEL BEING USED.
37. C
38. C 3) SET THE CORRECT LAG TIME TO THE VARIABLE 'TLAC'.
39. C
40. C 4) CHANGE THE ARRAYS QNC(I), QND(I), QNF(I), AND
41. C QG(I) TO THE APPROPRIATE MAXIMUM VALUES FOR FLOW
42. C RATES IN THE UNIT A-C, D, E, AND TOTAL AREA
43. C RESPECTIVELY.
44. C
45. C 5) CHANGE THE DATA AT THE END OF THE PROGRAM. THE FIRST
46. C 14 ROWS OF DATA CORRESPOND TO PAST GROSS FLOW RATES IN
47. C UNITS 1-8, 11, AND 15 RESPECTIVELY. THE CORRESPONDING
48. C ARRAYS ARE QGC(I), QGD(I), AND QGF(I). THE LAST
49. C 8 ROWS OF DATA CORRESPOND TO FUTURE EXPECTED FLOW
50. C RATES IN UNITS A-C, D, E. THE FIRST COLUMN
51. C FOR ALL 22 ROWS OF DATA IS THE TIME PERIOD IN MONTHS
52. C FOR EACH ROW OF FLOW RATES.
53. C
54. C 6) SET 'DELIV' EQUAL TO THE TOTAL NUMBER OF FUTURE WELLS
55. C PREDICTED FOR THE PRESSURE CELL.
56. C
57. C
58. C
59. C
60. C

```

```

61. C*****
62. C
63. C
64. C          DESCRIPTION OF VARIABLES AND ARRAYS
65. C
66. C
67. C
68. C      A, B, C, D, E = MULTIPLE LINEAR REGRESSION CONSTANTS
69. C                    CALCULATED IN THE RESERVES MODEL
70. C
71. C      DELIV = MAXIMUM NUMBER OF WELLS PREDICTED FOR THE RESERVOIR
72. C
73. C      P, G = LINEAR REGRESSION CONSTANTS FROM THE EMPIRICAL
74. C          POWER LAW EQUATION, RELATING DELTA (P/Z) FLOW
75. C          WITH Q-PQ AND (P/Z) TOP.
76. C
77. C      K = A VARIABLE USED IN SUBROUTINE SHIFT TO PICK THE CORRECT
78. C          POSITION IN THE APRAYS RMN(J), QNC(I),
79. C          QND(I), AND QNF(I).
80. C
81. C      TEST = TESTS WHETHER THE DELIVERABILITY PART OF THE MODEL
82. C            WILL BE USED.
83. C
84. C      TLAG = THE LAG TIME
85. C
86. C
87. C      DPS(I) = DELTA P SQUARED: THP DIFFERENCE BETWEEN TR2 SQUARE
88. C              OF THE PRESSURE IN THE RESERVOIR AND THE SQUARE OF
89. C              THE PRESSURE AT THE INLET TO THE POWER PLANT.
90. C
91. C      GP(I) = GROSS STEAM PRODUCED (10E9 LBS.)
92. C
93. C      QAVG(I) = AVERAGE FLOW RATE DURING TIME PERIOD.
94. C
95. C      QC(I) = FLOW RATE THAT IS COMPARED WITH AVERAGE FLOW
96. C             RATE TO DETERMINE WHETHER CONVERGENCE HAS BEEN
97. C             ACHIEVED.
98. C
99. C      QG(I) = THE PREDICTED GROSS PLGW RATE OF THE ENTIRE RESERVOIR.
100. C            DEPENDS ON THE RELATIVE AREAS OF THE UNITS CONTAINED
101. C            IN THE CELL.
102. C
103. C      ***+* *****
104. C            ALL FLOW RATES = (10E9 LBS./MO.) *****
105. C
106. C
107. C
108. C      QNC(I) = FUTURE GROSS FLOW RATE IN THE UNIT A-C AREA.
109. C
110. C      QND(I) = FUTURE GROSS FLOW RATE IN THE UNIT D AREA.
111. C
112. C      QNF(I) = FUTURE GROSS FLOW RATE IN THE UNIT F AREA.
113. C
114. C      QGC(I) = PAST GROSS FLOW RATE IN THE UNIT A-C AREA.
115. C
116. C      QGD(I) = PAST GROSS FLOW RATE IN THE UNIT D AREA.
117. C
118. C      QGF(I) = PAST GROSS FLOW RATE IN THE UNIT F AREA.
119. C
120. C      PZ1(I) = P/Z AT THE OLD ITERATION LEVEL.

```

```

121. C
122. C   PZ2(I) = P/Z AT THE NEW ITERATION LEVEL.
123. C
124. C   P(I) = PRESSURE
125. C
126. C   RM(I) = THE TIME STEP FOR PAST PLOY PERIODS. (MONTHS),
127. C
129. C   RMN(I) = TAP TIME PERIOD FOR FUTURE HOW PERIODS. (MO.)
129. C
130. C   WELLS(I) = THE NURBER OP WELLS AT SPECIFIC DATES. ASSUMES
131. C             THAT ENOUGH WELLS WILL HAVE BEEN DRILLED IN
132. C             THE FUTURE TO ALLOW THE NEEDED PLOY RATE,
133. C             UNTIL THE MAXIMUM NUMBER OP WELLS HAVE BEEN
134. C             DRILLED,
135. C
136. C   YEARS(I) = THE DATE IN YEARS.
137. C
138. C
139. C *****
140. C
141. C
142. C             SUBROUTINE VARIABLES
143. C
144. C
145. C   RMTDT = WPEPS 4 RUNNING COUNT OP THE PAST MONTHS WHICH
146. C             MUST BE USED TN TAE EQUIVALENT PLOY RATE CALCULATION.
147. C
148. C   QEQC = EQUIVALENT FLOW BATE IN THE UNIT A-C AREA.
149. C
150. C   QEQD = EQUIVALENT FLOW RATE IN THE UNIT D AREA.
151. C
152. C   QEQF = EQUIVALENT FLOW RATE IN THE UNIT F AREA.
153. C
154. C   TEST = A VAFIABLE THAT TESTS TO SEE IF THE LAG TIME
155. C             HAS BEEN EXCFEDED.
156. C ***** **
157. C * * **** ***** **
158. C   DIMENSION DPS(500),P(500),WELLS(40),PZE(500),QAVG(500),
159. C   1 QEND(500),QC(500),YFAR(100)
160. C   COMMON QEQC,QEQD,QEQF,QGC(500),QGD(500),QGF(500),RM(500),
161. C   1 RMN(500),QNC(500),QND(500),QNF(500),PZ1(500),PZ2(500),
162. C   2 QG(500),K,TLAG,GP(500)
163. C   YEAR(1)=22.0
164. C   YEAR(2)=23.0
165. C
166. C   SET THE LAG TIME FOUAL TO 30 MONTHS.
167. C
168. C   TLAG=30.0
169. C   TEST=1.0
170. C
171. C   ASSUMES 2.5 TIMES THE CURRENT DELIVERAEILTTY OF THE
172. C   RESERVOIR
173. C
174. C   DELIV=249.0
175. C   K=0
176. C   A=718.5
177. C   B=0.1544
176. C   C=71.2
179. C   D=436.7
180. C   E=717.4

```

```

181.          F=0.987
182.          G=0.257
183.          C
184.          C   SET THE FIRST PRESSURE EQUAL TO 540.
185.          C
186.          PZ1(1)=540.0
187.          GP(1)=360.2
188.          DO 10 I=2,79
189.          C
190.          C   THIS GIVES THE CATF EVERY 6 MONTHS.
191.          C
192.          YEAR(I+1)=YEAR(I)+0.5
193.          10 CONTINUE
194.          DO 20 I=1,14
195.          C
196.          C   READ IN THE PAST FLOW PATE CATA AT THE END OF PROGRAM.
197.          C
198.          READ(5,*) RM(I),QGC(I),QGD(I),QGF(I)
199.          20 CONTINUE
200.          DO 30 I=15,100
201.          RM(I)=0.0
202.          QGC(I)=0.0
203.          QGD(I)=0.0
204.          QGF(I)=0.0
205.          30 CONTINUE
206.          DO 40 I=1,8
207.          C
208.          C   READ IN THE FUTURE PREDICTED FLOW RATE BEHAVIOR.
209.          C
210.          READ(5,*) RMN(I),QNC(I),QND(I),QNF(I),QG(I)
211.          40 CONTINUE
212.          DO 50 I=9,500
213.          C
214.          C   FUTURE TIME PERIODS = 6 MONTHS.
215.          C
216.          RMN(I)=6.0
217.          C
218.          C   FUTURE MAXIMUM FLOW RATES PREDICTED FOR VARIOUS AREAS.
219.          C
220.          QNC(I)=2.975
221.          QND(I)=1.40
222.          QNF(I)=0.385
223.          QG(I)=4.76
224.          50 CONTINUE
225.          DO 90 I=1,400
226.          C
227.          C   COMPUTES FUTURE PRODUCTION ASSUMING A 25% RATE OF
228.          C   REPLACEMENT.
229.          C
230.          GP(I+1)=GP(I)+0.75*RMN(I)*QG(I)
231.          C
232.          C   SUBROUTINE SHIFT ADJUSTS TIME PERIODS AHEAD.  SUBROUTINE
233.          C   QEQUIV CALCULATES THE EQUIVALENT FLOW RATE FOR VARIOUS
234.          C   AREAS.
235.          C
236.          CALL SHIFT
237.          CALL QEQUIV
238.          C
239.          C   CALCULATE P/Z AT THE NEW LEVEL OF ITERATION UNTIL
240.          C   CONVERGENCE. PZ2 THEN BECOMES THE VALUE OF P/Z AT THE

```

```

241. C NEW LEVEL OF TIUF.
242. C
243. 60 PZ2(I) = A - B * GP(I+1) - C * (QEQC**P) / PZ1(I) **G - D * (QEQD**P) /
244. 1 PZ1(I) **G - E * (QEQE**P) / PZ1(I) **G
245. C
246. C THE CONVERGENCE CRITERIA IS A DIFFERENCE LESS THAN 0.1
247. C PSI.
248. C
249. C IF (ABS(PZ1(I) - PZ2(I)) .LT. 0.1) GO TO 70
250. PZ1(I) = PZ2(I)
251. GC TO 60
252. 70 IF (TEST.E2.0.0) SO TO 80
253. C
254. C CALCULATE PRESSURE USING VALUE OF P/Z AND ASSUMING
255. C A STRAIGHT LINE IN THE LOW PRESSURE REGION OF THE
256. C COMPRESSIBILITY (Z-FACTOR) CHARTS.
257. C
258. C P(I) = PZ2(I) * (1 - C.0002447 * PZ2(I))
259. C
260. C THE SQUARE OF 105 PSI, THE PRESSURE AT THE POWER PLANTS,
261. C IS EQUAL TO 11025.
262. C
263. C DPS(I) = P(I) ** 2 - 11025.0
264. C
265. C THIS IS THE NUMBER OF WELLS NEEDED TO SUSTAIN A
266. C DESIRED FLOW RATE UNTIL MAXIMUM NUMBER IS REACHED.
267. C
268. C WELLS(I) = 2G(I) * 5.54E+06 / DPS(I)
269. C IF (WELLS(I) .GT. DELIV) GO TO 210
270. 80 PZ1(I+1) = PZ2(I)
271. C IF (PZ2(I) .LT. 150) GO TO 100
272. 90 CONTINUE
273. 103 WRITE(6, 110)
274. 110 FORMAT(133(' '), //)
275. 120 WRITE(6, 130)
276. 133 FORMAT(20X, 'YEAR', 10X, 'GP NET (10E9 LBS)', 10X, 'P/Z TOP (PSI)')
277. C WRITE(6, 140)
278. 140 FORMAT(20X, 4(' '), 10X, 17(' '), 10X, 13(' '), //)
279. C DC 130 I=1, 400
280. C IF (PZ2(I) .LT. 150) GO TO 190
281. C IF (MOD(I, 25) .NE. 0) GO TO 160
282. C WRITE(6, 150)
283. 150 FORMAT(103(' '), /1H1, 100(' '), //)
284. C WRITE(6, 130)
285. C WRITE(6, 140)
286. 160 WRITE(6, 173) YEAR(I) GP(I+1), PZ2(I)
287. 170 FORMAT(19X, F6.1, 15X, F6.1, 20X, F5.1 /)
288. C
289. 183 CONTINUE
289. 193 WRITE(6, 200)
290. 203 FORMAT(103(' '), /1H1)
291. C GO TO 409
292. C
293. C THIS IS THE DELIVERABILITY PART OF THE MODEL. A TRIAL
294. C AND ERROR PROCEDURE IS USED TO CALCULATE FUTURE FLOW
295. C RATES. THIS IS DESCRIBED IN THE ACCOMPANYING REPORT.
296. C RAPID CONVERGENCE IS ACHIEVED IN 2 TO 4 ITERATIONS.
297. C
298. 210 WELLP = WELLS(I)
299. QEND(I) = QG(I)
300. QAVG(I+1) = QEND(I)

```

```

301.      PZ2 (I+1) = PZ2 (I)
302.      ISTART = I + 1
303.      IEND = I + 433
304.      DO 240 L = ISTART, IEND      --
305.      CALL SHIFT
306.      C
307.      C      THE PUTURE TIME PERIOD IS NOW ONLY ONE MONTH SO THAT
308.      C      THE PLOW RATE DECLINE: WILL BE SCOTHTER.
309.      C
310.      220  RM (1) = 1.0
311.      C
312.      C      FUTURE GROSS PLOW RATES IN SPECIFIC UNIT ABEAS WILL
313.      C      BE IN THE SAME PROPORTION AS BEFORE DECLINE BPGAN.
314.      C
315.      QGC (1) = QNC (9) * QAVG (L) / QG (9)
316.      QGD (1) = QND (9) * QAVG (L) / QG (9)
317.      QGF (1) = QNF (9) * QAVG (L) / QG (9)
318.      CALL QEQUIV
319.      GP (L+1) = G? (L) + 0.75 * RM (1) * QAVG (L)
320.      C
321.      C      THIS IS THE TFIAL AND ERROR CALCULATION OF PLOW RATE.
322.      C
323.      PZE (L) = A - B * GP (L+1) - C * {QEQC**F} / PZ2 (I) **G - D * {QFQD**F} /
324.      I      PZ2 (I) **G - E * {QEQF**F} / PZ2 (L) **G
325.      C
326.      C      TO CONVERT FROM P/Z TO PRESSURE, ASSUME A LINEAR
327.      C      RELATIONSHIP ON THE Z-FACTOR CHARTS.
328.      C
329.      P (L) = PZE (L) * (1 - 0.0002447 * PZE (L))
330.      C
331.      C      11025 IS THE SQUAFF OF 105, P INLET.
332.      C
333.      DPS (L) = P (L) **2 - 11025.0
334.      QEND (L) = 3?S (L) * WELLIF / 5.54E+0h
335.      QC (L) = {QEND (L) + QEND (L-1)} / 2
336.      C
337.      C      CONVERGENCE CRITERIA POR THE PLOW RATE IS 4
338.      C      DIFPEREHCE OF 0.0 1 {10E9 LBS./MO.} .
339.      C
340.      IF (ABS (QC (L) - QAVG (L)) .LT. 0.01) GO TO 230
341.      QAVG (L) = QC (L)
342.      C
343.      C      ONCE CONVERGENCE IS REACHED, RESET VALUES OF QAVG AND PZ2.
344.      C
345.      PZ2 (L) = PZE (L)
346.      GG TO 220
347.      230  PZ2 (L+1) = PZE (L)
348.      QAVG (L+1) = QAVG (L)
349.      IF (YEAR (I + (L-1) / 6) .EQ. 55) GO TO 250
350.      240  CONTINUE
351.      250  WRITE (6, 260)
352.      260  FORMAT (130 ('-'), //)
353.      270  WRITE (6, 280)
354.      283  FORMAT (20X, 'YEAR', 10X, 'GP NPT (10E9 LBS)', 10X, 'P/Z TOP (PSI)',
355.      I      10X, 'PLOW PATE (10E9 LBS/MO) ')
356.      290  WRITE (6, 290)
357.      290  FORN A? (20X, 4 ('-'), 10X, 17 ('-'), 10X, 13 ('-'),
358.      110X, 23 ('-'), //)
359.      DO 330 L = 1, I
360.      IF (MOD (L, 26) .NE. 0) GO TO 310

```

```

361.      WRITE(6,300)
362.      300  FORMAT(130(' '),/1H1,130(' '),//)
363.      WRITE(6,230)
364.      WRITE(6,290)
365.      310  WRITE(6,320) YEAR(L),GP(L+1),PZ2(L),QG(L)
366.      320  FORMAT(19X,F6.1,15X,F6.1,20X,F5.1,22X,F4.2,/)
367.      330  CONTINUE
368.      ISTART=ISTART+5
369.      YEARS=YEAR(I)
370.      DO 360 L=ISTART,IEND,6
371.      YEARS=YEARS+0.5
372.      IF(YEARS.EQ.55.5) GO TO 370
373.      IF(MOD(I+(I-I)/6,26).NE.0) GO TO 350
374.      WRITE(6,340)
375.      340  FORMAT(130(' '),/1H1,130(' '),//)
376.      WRITE(6,230)
377.      WRITE(6,230)
378.      350  WRITE(6,320) YEARS,GP(I+1),PZ2(L),QAVG(L)
379.      360  CONTINUE
380.      WRITE(6,380) WFLP
381.      380  FORMAT(/,5X,'IT HAS BEEN ASSUMED THAT FUTURE DRILLING WILL PRODUCE
382.      1E A TOTAL OF ',F5.1,' WEELS IN THE OLD GEYSERS PRESSURE CELL
383.      2',//)
384.      WRITE(6,390)
385.      393  FORMAT(130(' '),/1H1)
386.      403  STOP
387.      END
388.      SUBROUTINE SHIFT
393.      C
390.      C THIS SUBROUTINE SIMPLY ADJUSTS THE ARRAYS BY ONE TIME PERIOD.
391.      C THIS IS DONE SO THAT A NEW EQUIVALENT FLOW CAN BE CALCULATED.
392.      C
393.      COMMON QEQC,QEQD,QEQF,QGC(500),QGD(500),QGF(500),RM(500),
394.      1      RMN(500),QNC(500),QND(500),QNF(500),PZ1(500),PZ2(500),
395.      2      QG(500),K,FLAG,GP(500)
396.      DO 10 I=1,70
397.      RM(72-I)=RM(71-I)
398.      QGC(72-I)=QGC(71-I)
399.      QGD(72-I)=QGD(71-I)
400.      QGF(72-I)=QGF(71-I)
401.      10  CONTINUE
402.      K=K+1
403.      RM(1)=RMN(K)
404.      QGC(1)=QNC(K)
405.      QGD(1)=QND(K)
406.      QGF(1)=QNF(K)
407.      RETURN
408.      END
409.      SUBROUTINE QEQU IV
410.      C
411.      C THIS SUBROUTINE CALCULATES EQUIVALENT FLOW RATES BY USING
412.      C THE DEVELOPED EQUATIONS IN THE ACCOMPANYING REPORT.
413.      C
414.      COMMON QEQC,QEQD,QEQF,QGC(500),QGD(500),QGF(500),RM(500),
415.      1      RMN(500),QNC(500),QND(500),QNF(500),PZ1(500),PZ2(500),
416.      2      QG(500),K,FLAG,GP(500)
417.      TEST=0.0
418.      RMTOT=0.0
419.      QEQC=0.0
420.      QEQD=0.3

```



```

421.      QEQF=0.0
u22.      DO 10 I=1,71
423.      TEST=TEST+RM(I)
424.      IF (TLAG.LT.TEST) GO TO 20 _
025.      10 CONTINUE
426.      20 N=I-1
427.      DO 30 J=1,N
428.      RMTOT=RMTOT+RM(J)
429.      QEQC=QEQC+(QGC(J)-QGC(J+1))*SQRT(RMTOT)
430.      QEQD=QEQD+(QGD(J)-QGD(J+1))*SQRT(RMTOT)
431.      QEQF=QEQF+(QGF(J)-QGF(J+1))*SQRT(RMTOT)
432.      30 CONTINUE
437.      QEQC=QEQC/SQRT(TLAG)+QGC(I)
434.      QEQD=QEQD/SQRT(TLAG)+QGD(I)
435.      QEQF=QEQF/SQRT(TLAG)+QGF(I)
436.      RETURN
437.      END
438.      C
439.      C   THE FIRST 14 ROWS ARE PAST DATA.  THESE NORMALLY
440.      C   WILL NOT BE CHANGED.  THE FINAL 8 ROWS ARE FUTURE
441.      C   ASSUMPTIONS OF FLOP RATE, AND THESE MUST BE CHANGED
442.      C   FOR ASSUMPTIONS CONCERNING AREA EXTENT OF THE RESERVOIR.
443.      C
444.      $DATA
445.      14.0, 2.74 3.71 0.25
446.      9.0, 2.76 0.65 0.220
447.      6.0, 2.54 0.68 0.16
448.      8.0, 2.38 0.55 0.13
449.      6.0, 2.51 0.64 0.13
453.      6.0, 1.43 0.74 0.100
451.      8.0, 2.63 0.79, 0.0
452.      10.3, 2.61 0.75, 0.0
453.      7.0, 2.48 0.62, 0.0
454.      8.0, 2.58 0.31, 0.0
455.      13.0, 2.64, 0.0, 0.0
456.      10.0, 2.66, 0.0, 0.0
457.      12.3, 1.75, 0.0, 0.0
058.      15.0, 1.17, 0.0, 0.0
459.      9.0, 2.8 0.7 0.21 3.71
460.      12.0, 2.8 0.7 0.21 3.71
461.      6.0, 2.3 1.4 0.21 4.41
462.      6.0, 2.8 1.4 0.21 4.41
463.      6.3, 2.8 1.4 0.21 4.41
464.      6.0, 2.8 1.4 0.21 4.41
465.      6.0, 2.8 1.4 0.21 4.41
466.      6.9, 2.8 1.4 0.21 4.41

```

<u>YEAR</u>	<u>GP NET (10E9 LBS)</u>	<u>E/Z TCP (PSI)</u>	<u>FLOW RATE (10E9 LBS/MO)</u>
22.0	382.5	526.2	3.71
23.0	415.8	521.5	3.71
23.5	435.7	489.4	4.41
24.0	455.5	474.0	4.41
24.5	475.4	460.8	4.41
25.3	495.2	449.0	4.41
25.5	515.1	438.1	4.41
26.0	534.9	434.6	4.41
26.5	556.3	415.9	4.76
27.0	577.8	405.7	4.76
27.5	539.2	396.5	4.76
28.0	620.6	388.8	4.76
28.5	642.0	381.2	4.76
29.0	663.4	377.2	4.76
29.5	684.9	373.3	4.76
30.0	706.1	371.0	4.71
30.5	727.1	363.9	4.65
31.0	747.9	367.1	4.61
31.5	768.5	365.6	4.57
32.0	789.0	364.2	4.53
32.5	809.3	362.8	4.50
33.0	829.4	361.3	4.46
33.5	849.4	359.9	4.43
34.0	869.2	358.4	4.39
34.5	888.8	356.9	4.35

<u>YEAR</u>	<u>GP UET (10E9 LBS)</u>	<u>E/Z TCP (PSI)</u>	<u>FLOW RATE (10E9 LBS/MO)</u>
35.3	908.3	355.5	4.32
35.5	927.6	354.1	4.28
36.0	946.8	352.7	9.25
36.5	965.8	351.2	4.21
37.9	984.7	349.6	4.18
37.5	1003.4	348.5	4.15
39.0	1022.0	347.1	4.11
38.5	1040.4	345.7	4.08
39.0	1058.6	344.4	4.05
39.5	1076.8	343.0	4.02
40.0	1094.7	341.7	3.90
40.5	1112.6	340.4	3.95
41.0	1130.2	339.0	3.92
41.5	1147.8	337.7	3.83
42.0	1165.2	336.4	3.66
42.5	1182.5	335.2	3.83
43.0	1199.6	333.5	3.79
43.5	1216.6	332.3	3.76
44.0	1233.5	331.0	3.73
44.5	1250.2	329.7	3.70
45.0	1266.9	328.5	3.67
45.5	1283.3	327.3	3.65
46.0	1299.7	326.0	3.62
46.5	1315.9	324.8	3.59
47.0	1332.0	323.6	3.56
47.5	1348.0	322.4	3.53

<u>YEAR</u>	<u>GP NET (10E9 LBS)</u>	<u>P/Z TCP (PSI)</u>	<u>FLOW RATE (10E9 LBS/MO)</u>
48.0	1363.8	321.2	3.51
48.5	1379.6	320.1	3.48
49.0	1395.2	318.9	3.45
49.5	1410.7	317.7	3.43
53.0	1426.1	316.6	3.40
50.5	1441.3	315.4	3.37
51.0	1456.4	314.3	3.35
51.5	1471.5	313.1	3.32
52.0	1486.4	312.9	3.30
52.5	1501.2	310.9	3.27
53.0	1515.9	309.9	3.25
53.5	1530.0	305.7	3.22
54.0	1544.9	307.6	3.20
54.5	1553.2	306.5	3.18
55.0	1573.5	305.4	3.15

HAS BEEN ASSUED THAT FUTURE DRILLING UILL PRODUCE A TOTAL OF 253.5 WLLS IN THE OLD GEYSERS PRESSURE CEL: